

Constructing ‘hair’ for the three charge hole

Samir D. Mathur¹, Ashish Saxena² and Yogesh Srivastava³

Department of Physics,
The Ohio State University,
Columbus, OH 43210, USA

Abstract

It has been found that the states of the 2-charge extremal D1-D5 system are given by smooth geometries that have no singularity and no horizon individually, but a ‘horizon’ does arise after ‘coarse-graining’. To see how this concept extends to the 3-charge extremal system, we construct a perturbation on the D1-D5 geometry that carries one unit of momentum charge P . The perturbation is found to be regular everywhere and normalizable, so we conclude that at least this state of the 3-charge system behaves like the 2-charge states. The solution is constructed by matching (to several orders) solutions in the inner and outer regions of the geometry. We conjecture the general form of ‘hair’ expected for the 3-charge system, and the nature of the interior of black holes in general.

¹mathur@mps.ohio-state.edu

²ashish@pacific.mps.ohio-state.edu

³yogesh@pacific.mps.ohio-state.edu

1 Introduction

The Bekenstein-Hawking entropy of a black hole is

$$S = \frac{A}{4G} \quad (1.1)$$

where A is the area of the horizon. Statistical mechanics then suggests that the hole should have e^S states. But where are these states? In this paper we suggest an answer to this question, and support our conjecture by a calculation related to the 3-charge extremal hole.

1.1 Black hole ‘hair’

String theory computations with extremal and near extremal systems have shown that D-brane states with the same charges and mass as the hole have precisely e^S states [1, 2]. If we increase the coupling g these states should give black holes [3]. At least for extremal holes supersymmetry tells us that we cannot gain or lose any states when we change g [4, 5]. We are thus forced to address the question: How do the e^S configurations differ from each other in the gravity description?

Early attempts to find ‘hair’ on black holes were based on looking for small perturbations in the metric and other fields while demanding smoothness at the horizon. One found no such perturbations – the energy in a small deformation of the black hole solution would flow off to infinity or fall into the singularity, and the hole would settle down to its unique metric again. But if we *had* found such hair at the horizon we would be faced with an even more curious difficulty. We would have a set of ‘microstates’ as pictured in Fig.1(b), each looking like a black hole but differing slightly from other members of the ensemble.

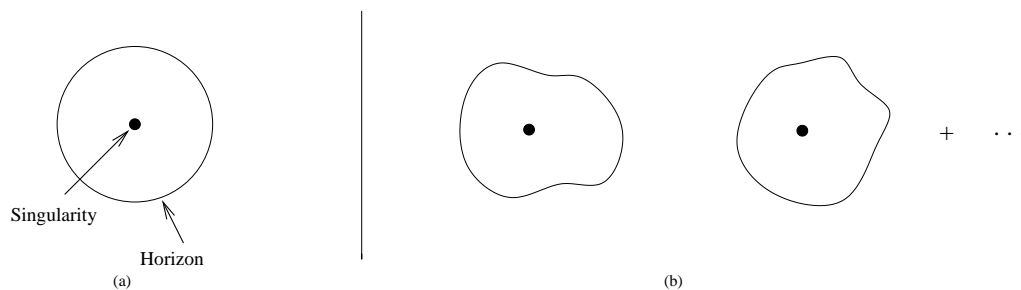


Figure 1: (a) The usual picture of a black hole. (b) If the microstates represented small deformations of (a) then each would itself have a horizon.

But if each microstate had a horizon as in the figure, then shouldn't we assign an entropy $\approx S$ to it? If we do, then we have e^S configurations, with *each* configuration having an entropy $\approx S$. This makes no sense – we wanted the microstates to *explain*

the entropy, not have further entropy themselves. This implies that if we do find the microstates in the gravity description, *then they should turn out to have no horizons themselves*.

We face exactly the same problem if we conjecture that the configurations all look like Fig.1(a) but differ from each other near the singularity; each configuration would again have a horizon, and thus an entropy e^S of its own.

The idea of *AdS/CFT* duality [6] adds a further twist to the problem. If string states at weak coupling become black holes at larger coupling, then one might think that the strings/branes are somehow sitting at the center $r = 0$ of the black hole. The low energy dynamics of the branes is a CFT. But the standard description of AdS/CFT duality says that the CFT is represented by a geometry that is *smooth* at $r = 0$ (Fig.2). In particular there are no sources or singularities near $r = 0$.

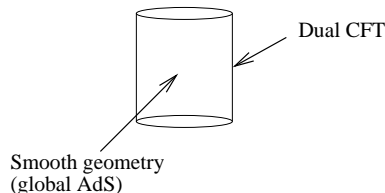


Figure 2: The D1-D5 CFT is represented by a *smooth* geometry in the dual representation.

Putting all this together suggests the following requirements for black hole ‘hair’:

- (a) There must be e^S states of the hole.
- (b) These individual states should have no horizon and no singularity.
- (c) ‘Coarse-graining’ over these states should give the notion of ‘entropy’ for the black hole.

This appears to be rather an extreme change in our picture of the black hole, particularly since (b) requires that the geometry of individual states differ significantly from the standard black hole metric everywhere in the interior of the hole, and not just within planck distance of the singularity.

Remarkably though, just such a picture of individual states was found for the 2-charge extremal D1-D5 system in [7][8]. We take n_5 D5 branes wrapped on $T^4 \times S^1$ bound to n_1 D1 branes wrapped on the S^1 . CFT considerations tell us that the entropy is $S_{micro} = 2\sqrt{2}\pi\sqrt{n_1 n_5}$, so the extremal ground state is highly degenerate. In the gravity description we should see the same number of configurations, except that in a classical computation this degeneracy would show up as a continuous family of geometries rather than discrete states. The *naive* metric that is usually written down for the D1-D5 state is pictured in Fig.3 – it goes to flat space at infinity, and heads to a singularity at $r = 0$. But a detailed analysis shows the following [7, 8]:

(a') The actual classical geometry of the extremal D1-D5 system is found to be given by a family of states parametrized by a vector function $\vec{F}(v)$; upon quantization this family of geometries should yield the $e^{2\sqrt{2}\pi\sqrt{n_1 n_5}}$ states expected from the entropy.

(b') Individual members of this family of states have no horizon and no singularity – we picture this in Fig.4.

(c') Suppose we define ‘coarse graining’ for a family of geometries in the following way. We draw a surface to separate the region where the metrics are all essentially similar from the region where they differ significantly from each other (indicated by the dashed line in Fig.5). The area A of this ‘horizon’ surface satisfies

$$S \approx \frac{A}{4G} \quad (1.2)$$

Note that the properties a',b',c' address directly the requirements a,b,c.

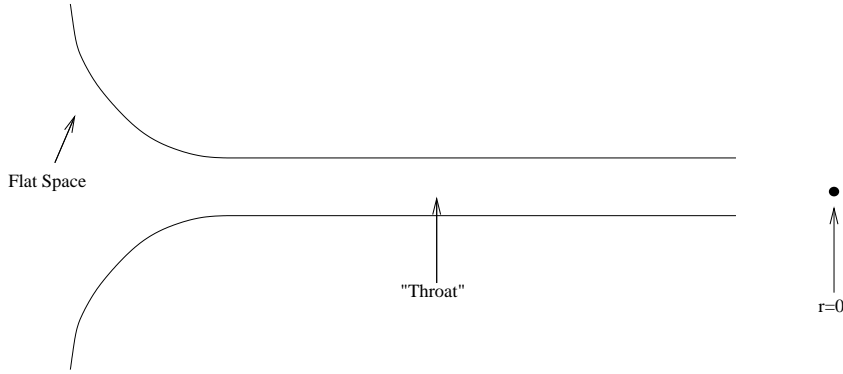


Figure 3: The *naive* geometry of the extremal D1-D5 system.

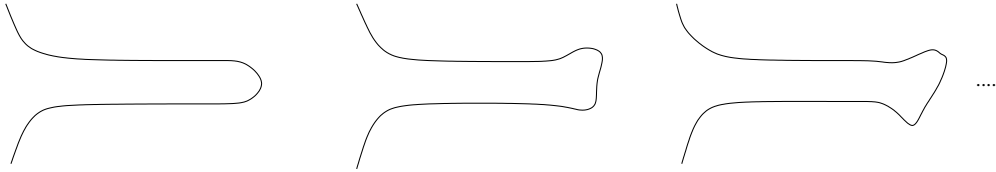


Figure 4: *Actual* geometries for different microstates of the extremal D1-D5 system.

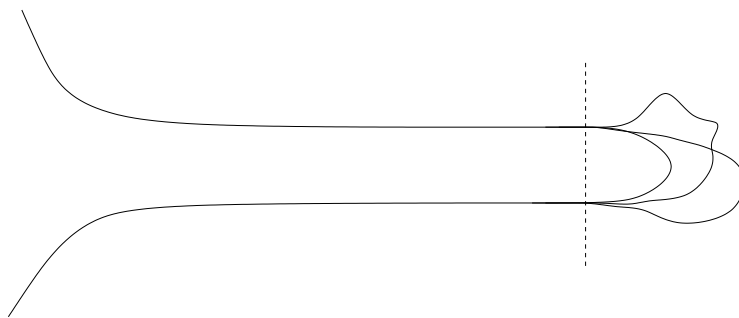


Figure 5: Obtaining the ‘horizon’ by ‘coarse-graining’.

1.2 The three charge case

The 2-charge D1-D5 extremal system has a ‘horizon’ whose radius is small compared to other length scales in the geometry, and the entropy of this system is determined from the geometry only upto a factor of order unity (this is the reason for the \approx sign in (1.2)). The 3-charge system which has D1, D5 and P charges (P is momentum along S^1) has a horizon radius that is of the same order as other scales in the geometry, and in the classical limit we get a Reissner-Nordstrom type black hole. The D-brane state entropy S_{micro} exactly equals S_{Bek} [1]. We would therefore like to find individual geometries that describe different states of the 3-charge hole. In line with what was said above, we expect a situation similar to that in Figs.3,4 – the *naive* D1-D5-P geometry has a horizon at $r = 0$, but *actual* geometries end smoothly (without horizon or singularity) before reaching $r = 0$.

If this description of the 3-charge hole were true then it would imply a simple consequence: There should be smooth perturbations of the 2-charge (D1-D5) system which add a small amount of the third (momentum) charge. Thus we should find small perturbations Ψ around the 2-charge geometries with the following properties

- (i) The perturbation has momentum p along the S^1 , which implies

$$\Psi \sim e^{i\frac{p}{R}y}, \quad p \in \mathbb{Z} \quad (1.3)$$

where y is the coordinate along S^1 and R is the radius of this S^1 .

- (ii) The perturbation takes the extremal 2-charge system to an extremal 3-charge so the energy of the perturbation should equal the momentum charge of the perturbation. This implies a t dependence

$$\Psi \sim e^{-i\omega t}, \quad \omega = \frac{p}{R} \quad (1.4)$$

- (iii) The perturbation must generate no singularity and no horizon, so it must be regular everywhere, and vanishing at $r \rightarrow \infty$ so as to be normalizable.

We start with a particular state of the 2-charge extremal system. We have a bound state of D1 and D5 branes, wrapped on a T^4 with volume $(2\pi)^4 V_4$ and an S^1 of radius R , sitting in asymptotically flat $4 + 1$ transverse spacetime. This system is in the Ramond (R) sector, which has many ground states. We pick the particular one (we call it $|0\rangle_R$) which if spectral flowed to the NS sector yields the NS vacuum $|0\rangle_{NS}$. The geometry for this 2-charge state is pictured in Fig.6. The radius of the S^3 in the region III is $(Q_1 Q_5)^{\frac{1}{4}}$. The parameter

$$\epsilon \equiv \frac{(Q_1 Q_5)^{\frac{1}{4}}}{R} \quad (1.5)$$

characterizes, roughly speaking, the ratio $\frac{\text{diameter}}{\text{length}}$ for the ‘throat’ region III.

In the NS sector we can act with a chiral primary operator on $|0\rangle_{NS}$. Let the resulting state be called $|\psi\rangle_{NS}$. The spectral flow of this state to the R sector gives a state $|\psi\rangle_R$; this will be an R ground state, and will have $L_0 = \bar{L}_0 = \frac{c}{24}$. We will construct the perturbation that will describe the CFT state

$$(J_{-1}^-)|\psi\rangle_R \quad (1.6)$$

This state has momentum charge $L_0 - \bar{L}_0 = 1$. We proceed in the following steps:

(A) The regions III and IV are actually a part of global $AdS_3 \times S^3 \times T^4$, and a coordinate change brings the metric here to the standard form [10, 11]. The wavefunction Ψ_{inner} for the state (1.6) in this region can be obtained by rotating a chiral primary perturbation in global $AdS_3 \times S^3$.

(B) We construct the appropriate wavefunction Ψ_{outer} in the regions I, II, III by solving the supergravity equations in this part of the geometry. We choose a solution that decays at infinity.

(C) We find that at leading order ϵ^0 the solutions Ψ_{inner} , Ψ_{outer} agree in the overlap region III.

(D) We extend the computation to order $\epsilon, \epsilon^2, \epsilon^3$ and continue to find agreement in the overlap region; this agreement appears to be highly nontrivial, and we take it as evidence for the existence of the solution satisfying (i), (ii), (iii) above.

After this computation we conclude with some conjectures about the form of ‘hair’ for generic states of the 3-charge hole, and a discussion of the physics underlying the new picture of the black hole interior that emerges from this structure of microstates.

2 The 2-charge system: review

In this section we review the results obtained earlier for the 2-charge D1-D5 system and describe the particular D1-D5 background to which we will add the perturbation carrying momentum charge P.

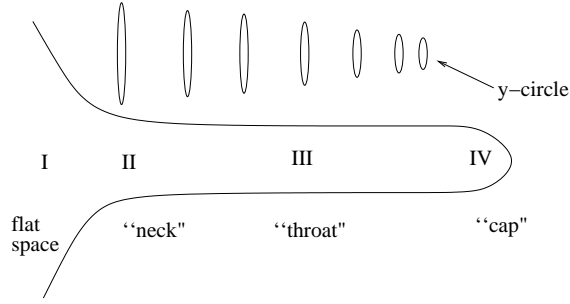


Figure 6: Different regimes of the starting 2-charge D1-D5 geometry.

2.1 Generating the ‘correct’ D1-D5 geometries

Consider IIB string theory compactified on $T^4 \times S^1$. The D1-D5 system can be mapped by a set of S, T dualities to the FP system

$$\begin{aligned} n_5 \text{ D5 branes along } T^4 \times S^1 &\rightarrow n_5 \text{ units of fundamental string winding along } S^1 \text{ (F)} \\ n_1 \text{ D1 branes along } S^1 &\rightarrow n_1 \text{ units of momentum along } S^1 \text{ (P)} \end{aligned}$$

The *naive* metric of the FP bound state in string frame is

$$ds^2 = -\left(1 + \frac{Q}{r^2}\right)^{-1} (dudv + \frac{Q'}{r^2} dv^2) + dx_i dx_i + dz_a dz_a \quad (2.1)$$

where $x_i, i = 1 \dots 4$ are the noncompact directions, $z_a, a = 1 \dots 4$ are the T^4 coordinates, and we have smeared all functions on T^4 . We will also use the definitions

$$u = t + y, \quad v = t - y \quad (2.2)$$

But in fact the bound state of the F and P charges corresponds to a fundamental string ‘multiwound’ n_5 times around S^1 , with all the momentum P being carried on this string as traveling waves. Since the F string has no longitudinal vibrations, these waves necessarily cause the strands of the multiwound string to bend away and separate from each other in the transverse directions. The possible configurations are parametrized by the transverse displacement $\vec{F}(v)$; we let this vibration be only in the noncompact directions x_1, x_2, x_3, x_4 . The resulting solution can be constructed using the techniques of [12, 13, 14], and we find for the metric in string frame [15]^{4,5}

$$\begin{aligned} ds^2 &= H(-dudv + Kdv^2 + 2A_i dx_i dv) + dx_i dx_i + dz_a dz_a \\ B_{vu} &= -G_{vu} = \frac{1}{2}H, \quad B_{vi} = -G_{vi} = -HA_i, \quad e^{-2\Phi} = H^{-1} \end{aligned} \quad (2.3)$$

⁴We can extend the construction to get additional states by letting the string vibrate along the T^4 directions; these states were constructed in [16].

⁵The angular momentum bounds of [15] and metrics found in [10, 11, 15] were reproduced in the duality related F-D0 system through ‘supertubes’ [18]. While supertubes help us to understand some features of the physics we still find that to construct metrics of general bound states of 2-charges and to identify the metrics with their CFT dual states the best way is to start with the FP system.

where

$$H^{-1} = 1 + \frac{Q}{L} \int_0^L \frac{dv}{|\vec{x} - \vec{F}(v)|^2}, \quad K = \frac{Q}{L} \int_0^L \frac{dv(\dot{F}(v))^2}{|\vec{x} - \vec{F}(v)|^2}, \quad A_i = -\frac{Q}{L} \int_0^L \frac{dv\dot{F}_i(v)}{|\vec{x} - \vec{F}(v)|^2} \quad (2.4)$$

($L = 2\pi n_1 R$, the total length of the F string.⁶)

Undoing the S,T dualities we find the solutions describing the family of Ramond ground states of the D1-D5 system [7]

$$ds^2 = \sqrt{\frac{H}{1+K}} [-(dt - A_i dx^i)^2 + (dy + B_i dx^i)^2] + \sqrt{\frac{1+K}{H}} dx_i dx_i + \sqrt{H(1+K)} dz_a dz_a \quad (2.5)$$

$$\begin{aligned} e^{2\Phi} &= H(1+K), \quad C_{ti}^{(2)} = \frac{B_i}{1+K}, \quad C_{ty}^{(2)} = -\frac{K}{1+K} \\ C_{ij}^{(2)} &= -\frac{A_i}{1+K}, \quad C_{ij}^{(2)} = C_{ij} + \frac{A_i B_j - A_j B_i}{1+K} \end{aligned} \quad (2.6)$$

where B_i, C_{ij} are given by

$$dB = - *_4 dA, \quad dC = - *_4 dH^{-1} \quad (2.7)$$

and $*_4$ is the duality operation in the 4-d transverse space $x_1 \dots x_4$ using the flat metric $dx_i dx_i$. The functions H^{-1}, K, A_i are the same as the functions in (2.4)

It may appear the the solution (2.5) will be singular at the points $\vec{x} = \vec{F}(v)$, but it was found in [7] that this singularity reflects all incoming waves in a simple way. The explanation for this fact was pointed out in a nice calculation in [16] where it was shown that the singularity (for generic $\vec{F}(v)$) is a *coordinate* singularity; it is the same coordinate singularity as the one encountered at the origin of a Kaluza-Klein monopole [17].

The family of geometries (2.5) thus have the form pictured in Fig.4. These geometries are to be contrasted with the ‘naive’ geometry for the D1-D5 system

$$ds_{naive}^2 = \frac{1}{\sqrt{(1 + \frac{Q_1}{r^2})(1 + \frac{Q_5}{r^2})}} [-dt^2 + dy^2] + \sqrt{(1 + \frac{Q_1}{r^2})(1 + \frac{Q_5}{r^2})} dx_i dx_i + \sqrt{\frac{1 + \frac{Q_1}{r^2}}{1 + \frac{Q_5}{r^2}}} dz_a dz_a \quad (2.8)$$

The actual geometries (2.5) approximate this naive geometry everywhere except near the ‘cap’.

It is important to note that we can perform dynamical experiments with these different geometries that distinguish them from each other. In [7] the travel time Δt_{sugra} was

⁶Parameters like Q, R are not the same for the FP and D1-D5 systems – they are related by duality transforms. Here we have not used different symbols for the two systems to avoid cumbersome notation and the context should clarify what the parameters mean. For full details on the relations between parameters see [15, 7]).

computed for a waveform to travel down and back up the ‘throat’ for a 1-parameter family of such geometries. Different geometries in the family had different lengths for the ‘throat’ and thus different Δt_{sugra} . For each geometry we found

$$\Delta t_{sugra} = \Delta t_{CFT} \quad (2.9)$$

where Δt_{CFT} is the time taken for the corresponding excitation to travel once around the ‘effective string’ in the CFT state dual to the given geometry. Furthermore, the backreaction of the wave on the geometry was computed and shown to be small so that the gravity computation made sense.

In [8] a ‘horizon’ surface was constructed to separate the region where the geometries agreed with each other from the region where they differed, and it was observed that the entropy of microstates agreed with the Bekenstein entropy that one would associate to this surface⁷

$$S_{micro} \sim \frac{A}{4G} \quad (2.10)$$

Such an agreement was also found for the 1-parameter family of ‘rotating D1-D5 systems’ where the states in the system were constrained to have an angular momentum J . The horizon surfaces in these cases had the shape of a ‘doughnut’.

2.2 The geometry for $|0\rangle_R$

The geometry dual to the R sector state $|0\rangle_R$ (which results from the spectral flow of the NS vacuum $|0\rangle_{NS}$) is found by starting with the FP profile

$$f_1(v) = a \cos\left(\frac{v}{n_5 R}\right), \quad f_2(v) = a \sin\left(\frac{v}{n_5 R}\right), \quad f_3(v) = 0, \quad f_4(v) = 0 \quad (2.11)$$

and constructing the corresponding D1-D5 solution. The geometry for this case had arisen earlier in different studies in [9, 10, 11]. For simplicity we set

$$Q_1 = Q_5 \equiv Q \quad (2.12)$$

which gives the D1-D5 solution

$$\begin{aligned} ds^2 = & -\frac{1}{h}(dt^2 - dy^2) + hf(d\theta^2 + \frac{dr^2}{r^2 + a^2}) - \frac{2aQ}{hf}(\cos^2 \theta dy d\psi + \sin^2 \theta dt d\phi) \\ & + h[(r^2 + \frac{a^2 Q^2 \cos^2 \theta}{h^2 f^2}) \cos^2 \theta d\psi^2 + (r^2 + a^2 - \frac{a^2 Q^2 \sin^2 \theta}{h^2 f^2}) \sin^2 \theta d\phi^2] + dz_a dz_a \end{aligned} \quad (2.13)$$

⁷In [5] the naive geometry for FP was considered, and it was argued that since the curvature became order string scale below some $r = r_0$, a ‘stretched horizon’ should be placed at r_0 . The area A of this stretched horizon also satisfied $\frac{A}{4G} \sim S_{micro}$. It is unclear, however, how this criterion for a ‘horizon’ can be used for the duality related D1-D5 system, where the geometry for small r is locally $AdS_3 \times S^3$ and the curvature is *constant* (and small). We, on the other hand have observed that geometries for different microstates *depart* from each other for $r \leq r_0$ and placed the horizon at this location; this gives the same horizon location for all systems related by duality.

where

$$a = \frac{Q}{R}, \quad f = r^2 + a^2 \cos^2 \theta, \quad h = 1 + \frac{Q}{f} \quad (2.14)$$

The dilaton and RR field are

$$\begin{aligned} e^{2\Phi} &= 1, & C_{ty}^{(2)} &= -\frac{Q}{Q+f}, & C_{t\psi}^{(2)} &= -\frac{Qa \cos^2 \theta}{Q+f} \\ C_{y\phi}^{(2)} &= -\frac{Qa \sin^2 \theta}{Q+f}, & C_{\phi\psi}^{(2)} &= Q \cos^2 \theta + \frac{Qa^2 \sin^2 \theta \cos^2 \theta}{Q+f} \end{aligned} \quad (2.15)$$

To construct the 3-charge solution below we will assume that

$$\epsilon \equiv \frac{a}{\sqrt{Q}} = \frac{\sqrt{Q}}{R} \ll 1 \quad (2.16)$$

which can be achieved by taking the compactification radius R to be large for fixed values of $\alpha', g, n_1, n_5, V_4$. In what follows we will ignore the T^4 and write 6-d metrics only. Since the dilaton Φ and T^4 volume are constant in the above solution the 6-d Einstein metric is the same as the 6-d string metric.

2.2.1 The ‘inner’ region

For

$$r \ll \sqrt{Q} \quad (2.17)$$

the geometry (2.13) becomes

$$\begin{aligned} ds^2 &= -\frac{(r^2 + a^2 \cos^2 \theta)}{Q}(dt^2 - dy^2) + Q(d\theta^2 + \frac{dr^2}{r^2 + a^2}) \\ &\quad - 2a(\cos^2 \theta dy d\psi + \sin^2 \theta dt d\phi) + Q(\cos^2 \theta d\psi^2 + \sin^2 \theta d\phi^2) \end{aligned} \quad (2.18)$$

The change of coordinates

$$\psi_{NS} = \psi - \frac{a}{Q}y, \quad \phi_{NS} = \phi - \frac{a}{Q}t \quad (2.19)$$

brings (2.18) to the form $AdS_3 \times S^3$

$$ds^2 = -\frac{(r^2 + a^2)}{Q}dt^2 + \frac{r^2}{Q}dy^2 + Q\frac{dr^2}{r^2 + a^2} + Q(d\theta^2 + \cos^2 \theta d\psi_{NS}^2 + \sin^2 \theta d\phi_{NS}^2) \quad (2.20)$$

We will call the region (2.17) the *inner region* of the complete geometry (2.13).

2.2.2 The ‘outer’ region

The region

$$a \ll r < \infty \quad (2.21)$$

is flat space ($r \rightarrow \infty$) going over to the ‘Poincare patch’ (with $y \rightarrow y + 2\pi R$ identification)

$$ds^2 = -\frac{r^2}{Q+r^2}(dt^2 - dy^2) + (Q+r^2)\frac{dr^2}{r^2} + (Q+r^2)[d\theta^2 + \cos^2\theta d\psi^2 + \sin^2\theta d\phi^2] \quad (2.22)$$

We will call the region (2.21) the *outer region* of the geometry (2.13). The inner and outer regions have a domain of overlap

$$a \ll r \ll \sqrt{Q} \quad (2.23)$$

2.2.3 The spectral flow map

The coordinate transformation (2.19) taking (2.18) to (2.20) gives *spectral flow* [10, 11]. The fermions of the supergravity theory are periodic around the S^1 parametrized by the coordinate y in (2.18), but the transformation (2.19) causes the S^3 to rotate once as we go around this S^1 , and the spin of the fermions under the rotation group of this S^3 makes them antiperiodic around y in the metric (2.20). Thus the metric (2.18) gives the dual field theory in the R sector while the metric (2.20) describes the CFT in the NS sector.

3 The perturbation carrying momentum

3.1 The equations

The fields of IIB supergravity in 10-d give rise to a large number of fields after reduction to 6-d. At the same time we get an enhancement of the symmetry group, as various different fields combine into larger representations of the 6-d theory.⁸ In [19] general 4b supergravities in 6-d were studied around $AdS_3 \times S^3$; their perturbation equations however apply to the more general background that we will use. These supergravities have the graviton g_{MN} , self-dual 2-form fields $C_{MN}^i, i = 1 \dots 5$, anti-self-dual 2-forms $B_{MN}^r, r = 1 \dots n$ and scalars ϕ^{ir} .

Suppose we have a solution to the field equations with a nontrivial value for the metric and one of the self-dual fields

$$g_{MN} = \bar{g}_{MN}, \quad C_{MN}^1 = \bar{C}_{MN}^1 \equiv C_{MN} \quad (3.1)$$

The choice $Q_1 = Q_5 = Q$ has made the field $C^{(2)}$ in (2.15) self-dual, and gives us such a background. (This choice simplifies the computations, but we expect that the perturbation we are constructing will exist for general Q_1, Q_5 as well.)

⁸In the actual reduction of IIB from 10-d to 6-d we also get additional fields like $A_\mu \equiv h_{a\mu}$, where $a = 1 \dots 4$ is a T^4 direction. We do not study these additional fields here.

Linear perturbations around the background (3.1) separate into different sets. The anti-self-dual field B_{MN}^r mixes only with the scalar ϕ^{1r} . We set $r = 1$ using the $SO(n)$ symmetry of the theory and write

$$B_{MN}^1 \equiv B_{MN}, \quad F_{MNP} = \partial_M B_{NP} + \partial_N B_{PM} + \partial_P B_{MN}, \quad \phi^{11} \equiv w \quad (3.2)$$

The field equations are⁹ (we write $\bar{H}_{MNP} = \partial_M \bar{C}_{NP} + \partial_N \bar{C}_{PM} + \partial_P \bar{C}_{MN}$)

$$F_{ABC} + \frac{1}{3!} \epsilon_{ABCDEF} F^{DEF} + w \bar{H}_{ABC} = 0 \quad (3.3)$$

$$w_{;A}{}^{;A} - \frac{1}{3} \bar{H}^{ABC} F_{ABC} = 0 \quad (3.4)$$

3.2 The (B, w) perturbation at leading order ($O(\epsilon^0)$)

In this subsection we construct the desired perturbation to leading order in the inner and outer regions and observe their agreement at this order of approximation.

3.2.1 Inner region: The chiral primary $|\psi\rangle_{NS}$

Consider the equations (3.3), (3.4) in the inner region. In the coordinates (2.20) this region is seen to be just ‘global’ $AdS_3 \times S^3$. We use $a, b \dots$ to denote indices on S^3 and $\mu, \nu \dots$ to denote indices on AdS_3 . We find the following solution for these equations in global $AdS_3 \times S^3$

$$w = \frac{e^{-2i\frac{a}{Q}lt}}{Q(r^2 + a^2)^l} \hat{Y}_{NS}^{(l)} \quad (3.5)$$

$$B_{ab} = B \epsilon_{abc} \partial^c \hat{Y}_{NS}^{(l)}, \quad B_{\mu\nu} = \frac{1}{\sqrt{Q}} \epsilon_{\mu\nu\lambda} \partial^\lambda B \hat{Y}_{NS}^{(l)} \quad (3.6)$$

where

$$\hat{Y}_{NS}^{(l)} = (Y_{(l,l)}^{(l,l)})_{NS} = \sqrt{\frac{2l+1}{2}} \frac{e^{-2il\phi_{NS}}}{\pi} \sin^{2l} \theta, \quad B = \frac{1}{4l} \frac{e^{-2i\frac{a}{Q}lt}}{(r^2 + a^2)^l} \quad (3.7)$$

In (3.6) the tensors ϵ_{abc}, g^{ab} etc are defined using the metric on an S^3 with *unit* radius. This choice simplifies the presentation of spherical harmonics but results in the factor (radius of S^3)⁻¹ = $\frac{1}{\sqrt{Q}}$ in the definition of $B_{\mu\nu}$. The tensors $\epsilon_{\mu\nu\lambda}, g^{\mu\nu}$ etc. are defined using the t, y, r part of the metric (2.20).¹⁰

⁹Our 2-form fields are twice the 2-form fields in [19]. Our normalizations agree with those conventionally used for the 10-D supergravity fields where the action is $-\frac{1}{12} \int F^2$.

¹⁰The spherical harmonics are representations of $so(4) \approx su(2) \times su(2)$; the upper labels in $Y_{(l,l)}^{(l,l)}$ give the j values in each $su(2)$, and the lower indices give the j_3 values. Thus $l = 0, \frac{1}{2}, 1, \dots$. The subscript NS on Y indicates that the arguments are the sphere coordinates in the NS sector, $(\theta, \psi_{NS}, \phi_{NS})$. When we write no such subscript it is to be assumed that the arguments of the spherical harmonic are the R sector coordinates (θ, ψ, ϕ) . More details about spherical harmonics are given in Appendix A.

This solution represents a chiral primary of the dual CFT [20]. To see this note the AdS/CFT relations giving charges and dimensions of bulk excitations

$$J_z^{NS} = \frac{i}{2}[\partial_{\psi_{NS}} + \partial_{\phi_{NS}}], \quad \bar{J}_z^{NS} = \frac{i}{2}[-\partial_{\psi_{NS}} + \partial_{\phi_{NS}}] \quad (3.8)$$

$$L_0^{NS} = i\frac{Q}{a}\partial_u, \quad \bar{L}_0^{NS} = i\frac{Q}{a}\partial_v \quad (3.9)$$

The solution (3.5)-(3.7) thus has

$$j^{NS} = l, \quad h^{NS} = l, \quad \bar{j}^{NS} = l, \quad \bar{h}^{NS} = l \quad (3.10)$$

which are the conditions for a chiral primary.

The coordinate transformation (2.19) brings us to the R sector. The scalar in these coordinates is

$$w = \frac{1}{Q(r^2 + a^2)^l} \hat{Y}^{(l)}, \quad \hat{Y}^{(l)} = \sqrt{\frac{2l+1}{2}} \frac{e^{-2il\phi}}{\pi} \sin^{2l} \theta \quad (3.11)$$

so that it has no t or y dependence. The components of B_{AB} similarly do not have any t, y dependence.

The dimensions in the R sector are given by (the partial derivatives this time are with respect to the R sector variables)

$$L_0 = i\frac{Q}{a}\partial_u, \quad \bar{L}_0 = i\frac{Q}{a}\partial_v \quad (3.12)$$

so that we get for our perturbation

$$h = \bar{h} = 0 \quad (3.13)$$

which is expected, since a chiral primary of the NS sector maps under spectral flow to a ground state of the R sector.¹¹

Let the CFT state dual to the perturbation (3.5)-(3.7) be called $|\psi\rangle_{NS}$, and let $|\psi\rangle_R$ be its image under spectral flow to the Ramond sector.

3.2.2 Inner region: The state $J_0^- |\psi\rangle_{NS} \leftrightarrow J_{-1}^- |\psi\rangle_R$

Consider again the inner region in the NS sector coordinates (2.20). We now wish to make the perturbation dual to the NS sector state

$$J_0^- |\psi\rangle_{NS} \quad (3.14)$$

¹¹The full spectral flow relations are $h = h_{NS} - j_{NS} + \frac{c}{24}$, $j = j_{NS} - \frac{c}{12}$. Spectral flow of the background $|0\rangle_{NS}$ gives $h^0 = h_{NS}^0 - \frac{c}{24}$, $j^0 = j_{NS}^0 - \frac{c}{12}$, so for the perturbation the spectral flow relations are just $h = h_{NS} - j_{NS}$, $j = j_{NS}$.

Since the operator J_0^- in the NS sector is represented by just a simple rotation of the S^3 , we can immediately write down the bulk wavefunction dual to the above CFT state

$$w = \frac{e^{-2i\frac{a}{Q}lt}}{Q(r^2 + a^2)^l} Y_{NS}^{(l)} \quad (3.15)$$

$$B_{ab} = B\epsilon_{abc}\partial^c Y_{NS}^{(l)}, \quad B_{\mu\nu} = \frac{1}{\sqrt{Q}}\epsilon_{\mu\nu\lambda}\partial^\lambda B Y_{NS}^{(l)} \quad (3.16)$$

$$Y_{NS}^{(l)} = (Y_{(l-1,l)}^{(l,l)})_{NS} = -\frac{\sqrt{l(2l+1)}}{\pi} \sin^{2l-1} \theta \cos \theta e^{i(-2l+1)\phi_{NS} + i\psi_{NS}}, \quad B = \frac{1}{4l} \frac{e^{-2i\frac{a}{Q}lt}}{(r^2 + a^2)^l} \quad (3.17)$$

This perturbation has

$$j_{NS} = l - 1, \quad \bar{j}_{NS} = l, \quad h_{NS} = l, \quad \bar{h}_{NS} = l \quad (3.18)$$

The spectral flow to the R sector coordinates should give

$$h = h_{NS} - j_{NS} = 1, \quad \bar{h} = \bar{h}_{NS} - \bar{j}_{NS} = 0 \quad (3.19)$$

so that we have a state with nonzero $L_0 - \bar{L}_0$, which means that it is a state with momentum. This can be seen explicitly by writing the solution (3.15)-(3.17) in the R sector coordinates. Writing

$$Y^{(l)} = -\frac{\sqrt{l(2l+1)}}{\pi} e^{i(-2l+1)\phi + i\psi} \sin^{2l-1} \theta \cos \theta, \quad u = t + y \quad (3.20)$$

we get

$$w = \frac{1}{Q} \frac{e^{-i\frac{a}{Q}u}}{(r^2 + a^2)^l} Y^{(l)} \quad (3.21)$$

$$B_{\theta\psi} = \frac{1}{4l} \frac{e^{-i\frac{a}{Q}u}}{(r^2 + a^2)^l} \cot \theta \partial_\phi Y^{(l)} \quad (3.22)$$

$$B_{\theta\phi} = -\frac{1}{4l} \frac{e^{-i\frac{a}{Q}u}}{(r^2 + a^2)^l} \tan \theta \partial_\psi Y^{(l)} \quad (3.23)$$

$$B_{\psi\phi} = \frac{1}{4l} \frac{e^{-i\frac{a}{Q}u}}{(r^2 + a^2)^l} \sin \theta \cos \theta \partial_\theta Y^{(l)} \quad (3.24)$$

$$B_{t\theta} = -\frac{a}{4l} \frac{e^{-i\frac{a}{Q}u}}{Q(r^2 + a^2)^l} \tan \theta \partial_\psi Y^{(l)} \quad (3.25)$$

$$B_{t\psi} = \frac{a}{4l} \frac{e^{-i\frac{a}{Q}u}}{Q(r^2 + a^2)^l} \sin \theta \cos \theta \partial_\theta Y^{(l)} \quad (3.26)$$

$$B_{y\theta} = \frac{a}{4l} \frac{e^{-i\frac{a}{Q}u}}{Q(r^2 + a^2)^l} \cot \theta \partial_\phi Y^{(l)} \quad (3.27)$$

$$B_{y\phi} = -\frac{a}{4l} \frac{e^{-i\frac{a}{Q}u}}{Q(r^2 + a^2)^l} \sin \theta \cos \theta \partial_\theta Y^{(l)} \quad (3.28)$$

$$B_{ty} = -\frac{1}{2Q^2} \frac{r^2 e^{-i\frac{a}{Q}u}}{(a^2 + r^2)^l} Y^{(l)} \quad (3.29)$$

$$B_{yr} = \frac{i}{2Q} \frac{r e^{-i\frac{a}{Q}u}}{(r^2 + a^2)^{l+1}} Y^{(l)} \quad (3.30)$$

We see that all fields behave as $\sim e^{-i\omega t + i\lambda y}$ with $\omega = |\lambda|$, so we have a BPS perturbation adding a third charge (momentum $P = -1$) to the 2-charge D1-D5 background.

3.2.3 Outer region: Continuing the perturbation $J_{-1}^- |\psi\rangle_R$

We now wish to ask if this solution in the inner region continues out to asymptotic infinity, falling off in a way that makes it a normalizable perturbation. To do this we solve the perturbation equations (3.3),(3.4) in the outer region (2.22). Requiring decay at infinity, we find the solution

$$w = \frac{e^{-i\frac{a}{Q}u}}{(Q + r^2)r^{2l}} Y^{(l)} \quad (3.31)$$

$$B_{ab} = B\epsilon_{abc}\partial^c Y^{(l)}, \quad B_{\mu\nu} = \frac{1}{\sqrt{Q + r^2}}\epsilon_{\mu\nu\lambda}\partial^\lambda B Y^{(l)}, \quad B = \frac{1}{4l} \frac{e^{-i\frac{a}{Q}u}}{r^{2l}} \quad (3.32)$$

where we have chosen the same spherical harmonic $Y^{(l)}$ that appears in (3.20). Again ϵ_{abc}, g^{ab} etc. refer to the metric of a *unit* S^3 (this gives the factor $(\text{radius of } S^3)^{-1} = \frac{1}{\sqrt{Q+r^2}}$ in $B_{\mu\nu}$), while $\epsilon_{\mu\nu\lambda}, g^{\mu\nu}$ etc. refer to the t, y, r part of the metric (2.22). Writing explicit components, the above solution becomes

$$w = \frac{e^{-i\frac{a}{Q}u}}{(Q + r^2)r^{2l}} Y^{(l)} \quad (3.33)$$

$$B_{\theta\psi} = \frac{1}{4l} \frac{e^{-i\frac{a}{Q}u}}{r^{2l}} \cot \theta \partial_\phi Y^{(l)} \quad (3.34)$$

$$B_{\theta\phi} = -\frac{1}{4l} \frac{e^{-i\frac{a}{Q}u}}{r^{2l}} \tan \theta \partial_\psi Y^{(l)} \quad (3.35)$$

$$B_{\psi\phi} = \frac{1}{4l} \frac{e^{-i\frac{a}{Q}u}}{r^{2l}} \sin \theta \cos \theta \partial_\theta Y^{(l)} \quad (3.36)$$

$$B_{ty} = -\frac{1}{2(Q+r^2)^2} \frac{e^{-i\frac{a}{Q}u}}{r^{2l-2}} Y^{(l)} \quad (3.37)$$

$$B_{tr} = \frac{ia}{r^{2l+1}} \frac{1}{4lQ} e^{-i\frac{a}{Q}u} Y^{(l)} \quad (3.38)$$

$$B_{yr} = \frac{ia}{r^{2l+1}} \frac{1}{4lQ} e^{-i\frac{a}{Q}u} Y^{(l)} \quad (3.39)$$

3.2.4 Matching at leading order

We wish to see if the solutions in the inner and outer regions agree in the domain of overlap $a \ll r \ll Q$. In this region we have

$$\frac{a}{\sqrt{Q}} \ll \left\{ \frac{a}{r}, \frac{r}{\sqrt{Q}} \right\} \ll 1 \quad (3.40)$$

We can match the solutions around any r in the range $a \ll r \ll Q$. To help us organize our perturbation expansion we choose this matching region to be around the geometric mean of a, Q , so that

$$\frac{a}{r} \sim \frac{r}{\sqrt{Q}} \sim \epsilon^{\frac{1}{2}} \quad (3.41)$$

In this region the scalar w in the inner region (given by (3.21)) and in the outer region (given by (3.33)) both reduce to the same function

$$w = \frac{e^{-i\frac{a}{Q}u}}{Qr^{2l}} Y^{(l)} + \dots \quad (3.42)$$

so that we get the desired agreement at leading order. We can similarly compare B_{MN} , but note that since B_{MN} is a tensor the components of B_{MN} depend on the coordinate frame. To see the order of a given component B_{MN} we should construct the field strength $F = dB$ from this component and then look at the values of F in an orthonormal frame. For example

$$B_{ty} \rightarrow F_{\hat{t}\hat{y}\hat{r}} \equiv F_{tyr} (g^{tt})^{\frac{1}{2}} (g^{yy})^{\frac{1}{2}} (g^{rr})^{\frac{1}{2}} \sim \frac{1}{Q^{\frac{3}{2}} r^{2l}} \quad (3.43)$$

Note that $\bar{H}_{\hat{t}\hat{y}\hat{r}} \sim \frac{1}{\sqrt{Q}}$, so that the $F_{\hat{t}\hat{y}\hat{r}}$ in the above equation is of the same order as $w\bar{H}_{\hat{t}\hat{y}\hat{r}}$, and thus B_{ty} is a term which we will match at leading order.

We then find that the components surviving at leading order reduce to the following forms for both the inner and outer solutions

$$B_{\theta\psi} = \frac{1}{4l} \frac{e^{-i\frac{a}{Q}u}}{r^{2l}} \cot \theta \partial_\phi Y^{(l)} \quad (3.44)$$

$$B_{\theta\phi} = -\frac{1}{4l} \frac{e^{-i\frac{a}{Q}u}}{r^{2l}} \tan \theta \partial_\psi Y^{(l)} \quad (3.45)$$

$$B_{\psi\phi} = \frac{1}{4l} \frac{e^{-i\frac{a}{Q}u}}{r^{2l}} \sin \theta \cos \theta \partial_\theta Y^{(l)} \quad (3.46)$$

$$B_{ty} = -\frac{1}{2Q^2} \frac{r^2 e^{-i\frac{a}{Q}u}}{r^{2l}} Y^{(l)} \quad (3.47)$$

Other components like $B_{y\phi}$ which do not agree are seen to be higher order terms. We will find agreement for these after we correct the inner and outer region computations by higher order terms.

3.3 Nontriviality of the matching

Before proceeding to study the solutions and matching at higher orders in ϵ , we observe that the above match at leading order is itself nontrivial. The dimensional reduction from 10-d to 6-d also gives some massless scalars in 6-d

$$\square s = 0 \quad (3.48)$$

We show that for such a scalar we *cannot* get any solution that is regular everywhere and decaying at infinity. For the scalar s we can find in the inner region $AdS_3 \times S^3$ a solution analogous to (3.15) [21]

$$s = \frac{e^{-i(2l+2)\frac{a}{Q}t}}{(r^2 + a^2)^{l+1}} Y_{NS}^{(l)} \quad (3.49)$$

where we have chosen the same spherical harmonic as in (3.15). Since the scalar generates not a chiral primary but a supersymmetry descendent, we get instead of (3.18)

$$j_{NS} = l - 1, \quad \bar{j}_{NS} = l, \quad h_{NS} = l + 1, \quad \bar{h}_{NS} = l + 1 \quad (3.50)$$

The solution (3.49) falls off towards the boundary of AdS , but in the complete geometry (2.13) it will not be normalizable at infinity. Using R sector coordinates (which are natural at $r \rightarrow \infty$) we find that the t, y dependence is $e^{-i\omega t + i\lambda y} = e^{-i\frac{a}{Q}(3t+y)}$. At large r we then find from the wave equation (3.48) the behavior [22]

$$s \sim \frac{1}{r^{\frac{3}{2}}} e^{-i\frac{a}{Q}(3t+y)} \cos[2\sqrt{2}\frac{a}{Q}r + \text{const}] Y^{(l)} \quad (3.51)$$

The reason for the slowness of the falloff at large r is the following. Since $\omega > |\lambda|$, we find that at large r not all the energy in the perturbation is tied to the S^1 momentum, and the residual energy goes to radial motion; this causes the perturbation to leak away to asymptotic infinity at late times. Normalizability at infinity is thus seen to require

$$\omega = |\lambda| \quad (3.52)$$

If we impose (3.52) on the solution for s , then we see that the solution regular at $r = 0$ is

$$s \sim (r^2 + a^2)^l Y^{(l)} \quad (3.53)$$

For the choice (3.52) there are two solutions in the outer region with radial dependences

$$(i) \ s \sim r^{-(2l+2)}, \quad (ii) \ s \sim r^{2l} \quad (3.54)$$

but the inner region solution matches onto the *growing* solution (ii) of the outer region, and we again get no normalizable solution.¹²

Thus we see that it is quite nontrivial that for the (B, w) system of fields the normalizable solutions of the inner and outer regions match up at leading order. We will now proceed to check the matching to higher orders in ϵ .

4 Matching at the next order ($O(\epsilon)$)

We wish to develop a general perturbation scheme that will correct our solution to higher orders in ϵ . It turns out that the inner region solution does not get corrected in a nontrivial way at order ϵ . In this section we first explain the general scheme, then apply it to the outer region to get the $O(\epsilon)$ corrections, and then explain how to match these to the inner region solution so that the entire solution is established to $O(\epsilon)$.

4.1 The perturbation scheme

The ‘outer region’ of our geometry $r \gg a$ is described to leading order by the metric (2.22). We must now take into account the corrections that arise because the exact geometry (2.13) departs from this leading order form. In particular we get small ‘off-diagonal’ components $g_{\mu a}$ in the metric and also small components like $\bar{H}_{\mu\nu a}, \bar{H}_{\mu ab}$ of \bar{H}_{ABC} . We develop a systematic way to handle these corrections so that we will get the full solution as a series in ϵ .

We expand the background and perturbations as

$$g_{MN} = g_{MN}^0 + g_{MN}^1 \quad (4.1)$$

$$H = H_0 + H_1 \quad (4.2)$$

$$F = F_0 + F_1 \quad (4.3)$$

$$* = *_0 + *_1 \quad (4.4)$$

$$w = w_0 + w_1 \quad (4.5)$$

$$\nabla^2 = \nabla_0^2 + \nabla_1^2 \quad (4.6)$$

The metric g_{MN}^0 is the metric (2.22) we had written earlier for the outer region. To get g_{MN}^1 we take the difference between the full metric (2.13) and the outer region metric (2.22); since we are seeking only the order ϵ corrections at this stage we keep terms of order $\frac{a}{r}, \frac{a}{\sqrt{Q}}$ in g^1 and discard higher order corrections. Similarly we obtain \bar{H}^1 . The

¹²For $\omega = |\lambda|$ the scalar equation (3.48) can be exactly solved in terms of hypergeometric functions, and the non-existence of a normalizable solution can be explicitly seen.

operation $*_0$ is defined using the metric g^0 , and $*_1$ contains the corrections needed to give the $*$ operation in the full metric (upto the desired order of approximation). ∇_0^2 is the Laplacian on the metric g^0 and ∇_1^2 corrects this (to the desired accuracy) to the Laplacian on the full metric.

To illustrate the general approximation scheme it is convenient to write the perturbation equation (3.3) in form language

$$F + *F + w\bar{H} = 0 \quad (4.7)$$

Inserting the expansions (4.1)-(4.6) in (4.7),(3.4) we get

$$\begin{aligned} F_0 + *_0 F_0 + w_0 \bar{H}_0 &= 0 \\ \nabla_0^2 w_0 - \frac{1}{3} \bar{H}_0^{MNP} F_{0MNP} &= 0 \end{aligned} \quad (4.8)$$

$$\begin{aligned} F_1 + *_0 F_1 + w_1 \bar{H}_0 &= S \\ \nabla_0^2 w_1 - \frac{1}{3} \bar{H}_0^{MNP} F_{1MNP} &= S_w \end{aligned} \quad (4.9)$$

where S_w and S are defined by

$$\begin{aligned} S &= -w_0 \bar{H}_1 - *_1 F_0 \\ S_w &= -\nabla_1^2 w_0 + \frac{1}{3} \bar{H}_1^{MNP} F_{0MNP} \end{aligned} \quad (4.10)$$

Eqs.(4.8) are just the leading order equations that give the leading order solution found for the outer regions in the last section. Eqs.(4.9) give the first order corrections. Note that the LHS of these equations have the same form as the leading order equations, so we need to solve the same equations again but this time with source terms S, S_w . These source terms can be explicitly calculated from the background geometry and the leading order solution.

4.2 Expanding in spherical harmonics

Even though the problem does not have exact spherical symmetry, it is convenient to decompose fields into spherical harmonics on S^3 . The breaking of spherical symmetry is then manifested by the fact that higher order corrections to the leading order solution contain spherical harmonics that differ from the harmonic chosen at leading order. We write

$$w = e^{-i\frac{a}{Q}u} \tilde{w}^{I_1} Y^{I_1} \quad (4.11)$$

$$B_{\mu\nu} = e^{-i\frac{a}{Q}u} b_{\mu\nu}^{I_1} Y^{I_1} \quad (4.12)$$

$$B_{\mu a} = e^{-i\frac{a}{Q}u} b_{\mu}^{I_3} Y^{I_3} \quad (4.13)$$

$$B_{ab} = e^{-i\frac{a}{Q}u} b^{I_1}_{abc} \partial^c Y^{I_1} \quad (4.14)$$

The Y^{I_1} are normalized scalar spherical harmonics on the unit 3-sphere. Their orders can be described by writing the rotation group of S^3 as $so(4) = su(2) \times su(2)$. The Y^{I_1} are representations (l, l) of $su(2) \times su(2)$, with $l = 0, \frac{1}{2}, 1, \dots$. These harmonics satisfy

$$\nabla^2 Y^{I_1} = -C(I_1) Y^{I_1}, \quad C(I_1) = 4l(l+1) \quad (4.15)$$

$$\nabla_{[a} \nabla_{b]} Y^{I_1} = 0 \quad (4.16)$$

The $Y_a^{I_3}$ are normalized vector spherical harmonics. They fall into two classes, one with $su(2) \times su(2)$ representations $(l, l+1)$ and the other with $(l+1, l)$. (Again $l = 0, \frac{1}{2}, 1, \dots$) We have

$$\nabla^a Y_a^{I_3} = 0 \quad (4.17)$$

$$\nabla_a Y_b^{I_3} - \nabla_b Y_a^{I_3} = \zeta(I_3) \epsilon_{abc} Y^{I_3 c} \quad (4.18)$$

where

$$\zeta(I_3) = \begin{cases} -2(l+1), & I_3 = (l+1, l) \\ 2(l+1), & I_3 = (l, l+1) \end{cases} \quad (4.19)$$

More details on spherical harmonics are given in Appendix A.

4.3 Outer region: Solving for the first order corrections

Returning to the field equations (4.9), we compute the sources S , finding

$$\begin{aligned} S_{tr\theta} &= \frac{Q}{2(Q+r^2)^2} \frac{1}{r^{2l+1}} \partial_\psi Y^{I_1} \tan \theta e^{-i\frac{a}{Q}u} \\ S_{tr\psi} &= -\frac{Q}{(Q+r^2)^2} \frac{1}{2r^{2l+1}} \left[\sin \theta \cos \theta \partial_\theta Y^{I_1} + 2 \frac{(l+3)r^2 + (l+1)Q}{Q+r^2} Y^{I_1} \cos^2 \theta \right] e^{-i\frac{a}{Q}u} \\ S_{yr\theta} &= -\frac{Q}{2(Q+r^2)^2} \frac{1}{r^{2l+1}} \partial_\phi Y^{I_1} \cot \theta e^{-i\frac{a}{Q}u} \\ S_{yr\phi} &= \frac{Q}{(Q+r^2)^2} \frac{1}{2r^{2l+1}} \left[\sin \theta \cos \theta \partial_\theta Y^{I_1} - 2 \frac{(l+3)r^2 + (l+1)Q}{Q+r^2} Y^{I_1} \sin^2 \theta \right] e^{-i\frac{a}{Q}u} \end{aligned} \quad (4.20)$$

The source S_w is zero at this order.

We can decompose these sources into scalar and vector spherical harmonics

$$S_{\mu\nu a} = s_{\mu\nu}^{I_3} Y_a^{I_3} + t_{\mu\nu}^{I_1} \partial_a Y^{I_1} \quad (4.21)$$

Substituting this decomposition in (4.9) we get the equations

$$b_{1\mu\nu}^{I_1} - \frac{r}{Q+r^2} \tilde{\epsilon}_{\mu\nu\lambda} \partial^\lambda b_1^{I_1} = t_{\mu\nu}^{I_1} \quad (4.22)$$

$$\partial_t b_{1y}^{I_3} - \partial_y b_{1t}^{I_3} + \zeta(I_3) \frac{r^3}{(Q+r^2)^2} b_{1r}^{I_3} = 0 \quad (4.23)$$

$$\partial_r b_{1t}^{I_3} - \partial_t b_{1r}^{I_3} + \zeta(I_3) \frac{b_{1y}^{I_3}}{r} = s_{tr}^{I_3} \quad (4.24)$$

$$\partial_y b_{1r}^{I_3} - \partial_r b_{1y}^{I_3} - \zeta(I_3) \frac{b_{1t}^{I_3}}{r} = s_{ry}^{I_3} \quad (4.25)$$

$$\partial_r \left(\frac{r^3}{(Q+r^2)^2} \partial_r b_1^{I_1} \right) + \frac{r}{(Q+r^2)^2} [2Q \tilde{w}_1^{I_1} - C(I_1) b_1^{I_1}] = 0 \quad (4.26)$$

$$\frac{1}{r(Q+r^2)} \partial_r (r^3 \partial_r \tilde{w}_1^{I_1}) - \frac{C(I_1)}{(Q+r^2)} \tilde{w}_1^{I_1} - \frac{8Q}{(Q+r^2)^3} [Q \tilde{w}_1^{I_1} - C(I_1) b_1^{I_1}] = 0 \quad (4.27)$$

Eq.(4.22) yields $b_{\mu\nu}^{I_1}$ once we know $b_1^{I_1}$; the source components $t_{\mu\nu}^{I_1}$ are listed in Appendix B. Eqs.(4.26),(4.27) allow the trivial solution

$$b_1 = \tilde{w}_1 = 0 \quad (4.28)$$

which we adopt, since other solutions would just amount to shifting the leading order solution taken for b, w . Eq.(4.23) yields $b_r = 0$. Eqns.(4.24), (4.25) are nontrivial and yield the solution ($u = t + y$, $v = t - y$)

$$b_{1ua} = b_{1u}^{I_3} Y_a^{I_3} = \frac{ia}{2} \sqrt{\frac{l}{(2l+1)(l+1)}} \frac{Q}{r^{2l}(Q+r^2)^2} Y_a^{(l+1,l)} + \quad (4.29)$$

$$- \frac{ia}{4r^{2l}} \left(\sqrt{\frac{2l-1}{l(2l+1)}} \frac{Q}{(Q+r^2)^2} - \frac{1}{Q} \sqrt{\frac{4l^2-1}{l^3}} \right) Y_a^{(l-1,l)} \quad (4.30)$$

$$b_{1va} = \frac{ia}{4} \sqrt{\frac{1}{(l+1)}} \frac{Q}{r^{2l}(Q+r^2)^2} Y_a^{(l,l+1)} \quad (4.31)$$

4.4 Matching at order ϵ

4.4.1 The inner region solution to order ϵ

Above we have applied the general scheme (4.9) to find the outer region solution to order ϵ . In general we would have to apply a similar scheme to correct the inner region solution as well. But it turns out that the expansion in the inner region goes in powers of ϵ^2 . Since at this stage we are only matching terms of order ϵ^0, ϵ^1 we do not need to perform any extra computation for the inner region, and the solution (3.21)-(3.30) is already correct

to the desired order. But to effect the comparison with the outer region we perform two manipulations on the inner region solution. First we express the set $B_{ta} = \{B_{t\theta}, B_{t\psi}, B_{t\phi}\}$ and the set B_{ya} in terms of scalar and vector harmonics

$$\begin{aligned}
B_{ta} &= \frac{iae^{-i\frac{a}{Q}u}}{2Q(r^2+a^2)^l} \left[\frac{\sqrt{l}Y_a^{(l+1,l)}}{\sqrt{(2l+1)(l+1)}} + \frac{Y_a^{(l,l+1)}}{2\sqrt{l+1}} + \right. \\
&\quad \left. \frac{l+1}{2l} \sqrt{\frac{2l-1}{l(2l+1)}} Y_a^{(l-1,l)} + \frac{\partial_a Y^{(l)}}{4l^2(l+1)} \right] \\
B_{ya} &= \frac{iae^{-i\frac{a}{Q}u}}{2Q(r^2+a^2)^l} \left[\frac{\sqrt{l}Y_a^{(l+1,l)}}{\sqrt{(2l+1)(l+1)}} - \frac{Y_a^{(l,l+1)}}{2\sqrt{l+1}} + \right. \\
&\quad \left. \frac{l+1}{2l} \sqrt{\frac{2l-1}{l(2l+1)}} Y_a^{(l-1,l)} - \frac{(2l-1)\partial_a Y^{(l)}}{4l^2(l+1)} \right]
\end{aligned} \tag{4.32}$$

Next we perform a gauge transformation on B_{MN}

$$B_{MN} \rightarrow B_{MN} + \nabla_M \Lambda_N - \nabla_N \Lambda_M \tag{4.33}$$

Choosing

$$\Lambda_t = \frac{i}{8l^2(l+1)} \frac{a}{Q(r^2+a^2)^l} Y^{(l)} e^{-i\frac{a}{Q}u} \tag{4.34}$$

$$\Lambda_y = -\frac{i(2l-1)}{8l^2(l+1)} \frac{a}{Q(r^2+a^2)^l} Y^{(l)} e^{-i\frac{a}{Q}u} \tag{4.35}$$

we remove the components proportional to $\partial_a Y^{(l)}$ in (4.32), while getting additional terms in other components of B . In particular

$$B_{tr} = \frac{i}{4l(l+1)} \frac{ar}{Q(r^2+a^2)^{l+1}} Y^{(l)} e^{-i\frac{a}{Q}u} \approx \frac{i}{4l(l+1)} \frac{a}{Qr^{2l+1}} Y^{(l)} e^{-i\frac{a}{Q}u} \tag{4.36}$$

$$B_{yr} = \frac{i(2l^2+1)}{4l(l+1)} \frac{ar}{Q(r^2+a^2)^{l+1}} Y^{(l)} e^{-i\frac{a}{Q}u} \approx \frac{i(2l^2+1)}{4l(l+1)} \frac{a}{Qr^{2l+1}} Y^{(l)} e^{-i\frac{a}{Q}u} \tag{4.37}$$

We will see that with this gauge choice we will get a direct agreement of B_{MN} between the outer and inner regions.

4.4.2 The outer region solution to order ϵ

We had solved the field equations to first order in ϵ for the outer region in subsection (4.3) above. We list the complete solution thus obtained to order ϵ

$$\begin{aligned}
w &= \frac{e^{-i\frac{a}{Q}u}}{r^{2l}(Q+r^2)} Y^{(l)} \\
B_{\theta\psi} &= \frac{1}{4l} \frac{e^{-i\frac{a}{Q}u}}{r^{2l}} \cot \theta \partial_\phi Y^{(l)} \\
B_{\theta\phi} &= -\frac{1}{4l} \frac{e^{-i\frac{a}{Q}u}}{r^{2l}} \tan \theta \partial_\psi Y^{(l)} \\
B_{\psi\phi} &= \frac{1}{4l} \frac{e^{-i\frac{a}{Q}u}}{r^{2l}} \sin \theta \cos \theta \partial_\theta Y^{(l)} \\
B_{ty} &= -\frac{1}{2(Q+r^2)^2} \frac{e^{-i\frac{a}{Q}u}}{r^{2l-2}} Y^{(l)} \\
B_{tr} &= -\frac{ia}{r^{2l+1}} \left(\frac{Q}{(Q+r^2)^3} \frac{[(l+2)r^2 + lQ]}{4l(l+1)} - \frac{1}{4lQ} \right) Y^{(l)} e^{-i\frac{a}{Q}u} \\
B_{yr} &= \frac{ia}{r^{2l+1}} \left(\frac{(2l-1)Q}{(Q+r^2)^3} \frac{[(l+2)r^2 + lQ]}{4l(l+1)} + \frac{1}{4lQ} \right) Y^{(l)} e^{-i\frac{a}{Q}u} \\
B_{ta} &= \frac{iaQe^{-i\frac{a}{Q}u}}{2r^{2l}(Q+r^2)^2} \left[\sqrt{\frac{l}{(2l+1)(l+1)}} Y_a^{(l+1,l)} + \frac{Y_a^{(l,l+1)}}{2\sqrt{l+1}} - \frac{1}{2} \sqrt{\frac{2l-1}{l(2l+1)}} Y_a^{(l-1,l)} \right] \\
&\quad + \frac{ia}{4Qr^{2l}} \sqrt{\frac{4l^2-1}{l^3}} Y_a^{(l-1,l)} \\
B_{ya} &= \frac{iaQe^{-i\frac{a}{Q}u}}{2r^{2l}(Q+r^2)^2} \left[\sqrt{\frac{l}{(2l+1)(l+1)}} Y_a^{(l+1,l)} - \frac{Y_a^{(l,l+1)}}{2\sqrt{l+1}} - \frac{1}{2} \sqrt{\frac{2l-1}{l(2l+1)}} Y_a^{(l-1,l)} \right] \\
&\quad + \frac{ia}{4Qr^{2l}} \sqrt{\frac{4l^2-1}{l^3}} Y_a^{(l-1,l)}
\end{aligned} \tag{4.38}$$

4.4.3 Comparing the inner and outer solutions at order ϵ

In the region where we match solutions we have to substitute at the present order of approximation

$$\frac{1}{(r^2+a^2)^l} \approx \frac{1}{r^{2l}}, \quad \frac{1}{(Q+r^2)} \approx \frac{1}{Q} \tag{4.39}$$

We then find agreement between the inner region solution (in the gauge discussed above) and outer region solution (4.38).

5 Matching at higher orders

We follow the same scheme to extend the computation to higher orders in ϵ . At each stage the sources S, S_w get contributions from all the terms found at preceding orders.

The computations are straightforward though tedious, and most are done using symbolic manipulation programs.

The solutions obtained for the inner region are listed in Appendix **B**. We have given the solutions in the NS sector coordinates; they must be spectral flowed to the R sector and gauge transformations performed to see directly the agreement with the outer region solutions. As mentioned before the perturbation series in the NS sector of the inner region proceeds in even powers of ϵ , and the odd powers in ϵ result from the spectral flow (2.19).

The solutions obtained for the outer region are listed in Appendix **C**. These are already in R sector coordinates. Note that at each order when we solve the equations with sources we have to choose a homogeneous part to the solution as well, and these parts have been chosen to give regularity everywhere as well as agreement between the inner and outer regions.

We carry out the computation of the solution in each region to order $O(\epsilon^3)$. We find complete agreement between the inner and outer region solutions upto the order investigated. At each stage of the computation there is the possibility of finding that some field is growing at infinity, and it is very nontrivial that this does not happen for any field at any of the orders studied. Thus we expect that the exact solution does exist and is likely to be expressible in closed form.

At all the orders that we have investigated the scalar w can be seen to arise from expansion of the solution

$$w = \frac{e^{-i\frac{a}{Q}u}Y^{(l)}}{(r^2 + a^2)^l(Q + f)}, \quad f = r^2 + a^2 \cos^2 \theta \quad (5.1)$$

Note that this expression involves just the combinations $(r^2 + a^2), f$ which appear in the geometry (2.13). We do not have a similar compact expression for the B field; it is plausible that the compact form would require us to express this 2-form field as part 2-form and part 6-form (the magnetic dual representation). We hope to investigate this issue elsewhere.

6 Discussion

We have constructed regular, normalizable supergravity perturbations in the inner and outer regions by a process of successive corrections, and observed that at each order the solutions agree in the domain of overlap. This agreement is very nontrivial, and we take this as evidence for the existence of an exact solution to the problem – i.e. we expect that there exists a regular perturbation on the 2-charge D1-D5 geometry (2.13) which carries one unit of momentum charge and adds one unit of energy (thus yielding an extremal 3-charge solution). We now return to our initial discussion of black hole interiors, and the significance of this solution in that context.

The usual picture of a black hole has a horizon, a singularity at the center, and ‘empty space’ in between. Abstract arguments given in the introduction suggested a

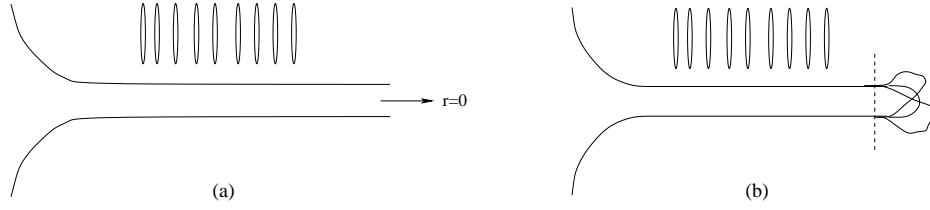


Figure 7: (a) Naive geometry for the 3-charge extremal system. (b) Expected structure for the system.

different picture where the interior was nontrivial and exhibited the degrees of freedom contributing to the entropy. The 2-charge extremal system turned out to look like this latter picture – its properties (a')-(c') listed in the introduction matched the suggested properties (a)-(c). What about the 3-charge extremal hole? This latter hole has become a benchmark system for understanding black holes, and any lessons deduced here likely extend to all holes in all dimensions.

The metric conventionally written for the D1-D5-P extremal system is

$$\begin{aligned}
 ds^2 = & \frac{1}{\sqrt{(1 + \frac{Q_1}{r^2})(1 + \frac{Q_5}{r^2})}} [-dudv + \frac{Q_p}{r^2} dv^2] \\
 & + \sqrt{(1 + \frac{Q_1}{r^2})(1 + \frac{Q_5}{r^2})} [dr^2 + r^2 d\Omega_3^2] + \sqrt{\frac{(1 + \frac{Q_1}{r^2})}{(1 + \frac{Q_5}{r^2})}} dz_a dz_a
 \end{aligned} \tag{6.1}$$

This is similar to the ‘naive’ metric (2.8) of the 2-charge D1-D5 extremal system, except that the y circle stabilizes to a fixed radius as $r \rightarrow 0$ instead of shrinking to zero size (we picture the geometry (6.1) in Fig.7(a)). The geometry (6.1) has a completion that it continues past the horizon at $r = 0$ to the ‘interior’ of the black hole, where we have a timelike singularity – the metric is just a 4+1 analogue of the extremal Reissner-Nordstrom black hole.

In a roughly similar manner one might have asked if the 2-charge metric continues past the ‘horizon’ $r = 0$ to another region, but here we do know the answer – the naive metric (2.8) is incorrect, and the actual geometries ‘cap off’ before reaching $r = 0$. We are therefore led to ask if a similar situation holds for the 3-charge system, so that the actual geometries ‘cap off’ before reaching $r = 0$ as in Fig.7(b). We would then draw the ‘horizon’ as a surface which bounds the region where the geometries differ from each other significantly; this surface is indicated by the dashed line in Fig.7(b). Note that for the 3-charge system the area of this ‘horizon’ will give *exactly*

$$\frac{A}{4G} = S_{micro} = 2\pi \sqrt{n_1 n_5 n_p} \tag{6.2}$$

This is because in the naive metric (6.1) the cross sectional area of the throat saturates to a constant A as $r \rightarrow 0$, and it is this same value A that will be picked up at the location

of the dashed line in Fig.7(b). But from [1] we know that this area A satisfies (6.2). (For the 2-charge case we could find A only upto a factor of order unity, since the y circle of the cross section was shrinking with r , and the natural uncertainty in the location of the ‘horizon surface’ leads to a corresponding uncertainty in A .)

Thus for the 3-charge system the nontrivial issue is not horizon area (which we see will work out anyway) but the nature of the geometry inside the horizon. The computation of this paper has indicated that if we have one unit of P then at least one extremal state

$$|\Psi\rangle = J_{-1}^-|0\rangle_R \quad (6.3)$$

of the 3-charge system is described by a geometry like Fig.7(b) and not by Fig.7(a). It may be argued though that the 2-charge extremal states and the state (6.3) are not sufficiently like generic black hole states to enable us to conclude that Fig.7(b) is the generic geometry of the 3-charge system. Here we give several arguments that counter this possibility:

(a) *Is the 2-charge system like a black hole?* It is sometimes argued that the 2-charge extremal system is not really a black hole since the horizon area vanishes classically. We argue against this view. The microscopic entropy of the 2-charge extremal system ($S=2\sqrt{2}\pi\sqrt{n_1n_5}$) arises by partitions of $N = n_1n_5$ in a manner similar to the entropy $2\pi\sqrt{n_1n_5n_p}$ of the 3-charge extremal system which arises from partitions of $N = n_1n_5n_p$. The ‘horizon’ that we have constructed for the 2-charge system satisfies $S \approx A/4G$, so this ‘horizon’ area is $\sim \sqrt{n_1n_5}$ times $(l_p)^3$, and is thus *not* small at all in planck units.

Why then do we think of this horizon as small? The 2-charge metric has factors like $\sim (1 + \frac{Q_1}{r^2}), (1 + \frac{Q_5}{r^2})$. Assuming $Q_1 \sim Q_5$ and $n_1 \sim n_5 \sim n$ we find that the geometry has a scale, the ‘charge radius’, which grows with n as $r \sim Q^{\frac{1}{2}} \sim n^{\frac{1}{2}}$. Since the horizon is a 3-dimensional surface, and we have found $S_{micro} \sim n \sim \frac{A}{4G}$, the horizon radius is $r \sim n^{\frac{1}{3}}$. Suppose we take the classical limit $n \rightarrow \infty$ and then scale the metric so that the charge radius is order unity. In this limit the horizon radius will *vanish*. For the 3-charge system, both the charge radius and the horizon radius behave as $r \sim n^{\frac{1}{2}}$, so the horizon radius remains nonzero in the analogous classical limit.

But this behavior of classical limits does not imply that the 2-charge system has an ignorable horizon – the horizon does give the correct entropy, and the presence of the other, larger, length scale appears irrelevant to the physics inside this horizon. The region $r \sim Q^{\frac{1}{2}}$ is far removed from the horizon region, and simply governs the changeover from ‘throat geometry’ to ‘flat space’.

(b) *Return time Δt_{CFT} :* For the 2-charge system, the naive metric is (2.8). If we throw a test particle down the throat of this naive metric, it does not return after any finite time. In the dual CFT however an excitation absorbed by the ‘effective string’ can be re-emitted after a time $\Delta t_{CFT} < \infty$. How do we resolve this contradiction? One might think that nonperturbative effects cause the test particle to turn back from some point in the throat of the naive geometry, but this cannot be the case since the return time Δt_{CFT} is different for different states of the 2-charge system (the length of the components of

the effective string are different for different states). The resolution of this puzzle was that the throats were capped; the cap was different for different states [7], and we get (2.9).

The CFT for the 3-charge system is described by the same effective string; we just have additional momentum excitations on the effective string. We would thus again have some finite time Δt_{CFT} after which an excitation should be emitted back from the system, and the requirement (2.9) then suggests that Fig.7(b) is the correct picture for the general states of the 3-charge system, rather than Fig.7(a).

(c) *Fractionation:* We have argued that the interior of the horizon is not the conventionally assumed ‘empty space with central singularity’. How can the classical expectation be false over such large length scales? The key physical effect is ‘fractionation’. If we excite a pair of left and right vibrations on a string of length L , the minimum excitation threshold is $\Delta E = \frac{2\pi}{L} + \frac{2\pi}{L} = \frac{4\pi}{L}$. But if we have a bound state of n strings, then we get one long string of length nL , and the threshold drops to $\frac{4\pi}{nL}$ [23]. If we start with 2-charges, n_1 D1 branes and n_5 D5 branes, then the excitations of the third charge, momentum, come in even smaller units, and $\Delta E = \frac{4\pi}{n_1 n_5 L}$ [24]. If we assume more generally that for the bound state of mutually supersymmetric branes the excitations always fractionate in this way, then we find that the excitations of the D1-D5-P hole are such that they extend to a radial distance that is just the horizon scale [25]. For the 2-charge FP where we have explicitly constructed all geometries this fractionation effect can be directly seen – because the momentum waves are fractionally moded on the multiply wound F string, the strands of the F string separate and spread over a significant transverse area, which extends all the way to the ‘horizon’.

(d) *Other 3-charge states:* The general perturbations around the 2-charge solution that we have chosen decompose into two classes: The antisymmetric field + scalar perturbations (which we have analyzed) and the metric + self-dual field perturbations. We have checked upto leading order (ϵ^0) that the latter class gives a regular solution as well. Further, the 2-charge solution that we started with may appear special (It has for instance angular momentum $\frac{n_1 n_5}{2}$ in each $su(2)$ factor, while the generic 2-charge state has negligible net angular momentum) but we have also checked that at leading order we get regular perturbations for all starting 2-charge geometries. In principle all these computations could be carried out to higher orders in ϵ , but the technical complexities would be greater due to less symmetry in the starting configuration.

(e) *Nonextremal holes:* Having found the above structure for extremal systems, we expect a similar structure for near extremal and also neutral holes, with the difference that the branes in the extremal systems are replaced by a collection of branes and anti-branes. Indeed, for the non-extremal D1-D5-P system it is known that the entropy of holes arbitrarily far from extremality can be reproduced exactly if we assume that the energy is optimally partitioned between branes and anti-branes while reproducing the overall charges and mass [26].

In an interesting recent paper [27] it was argued that the ‘black ring’ solutions car-

rying D1-D5-P charges (plus nonextremality) had pathologies like closed timelike curves and thus it was not possible to add momentum to general rotating D1-D5 states. Our construction, on the other hand *does* take a D1-D5 state with some angular momentum, and adds one unit of momentum. How do we reconcile these different conclusions?

The construction of [27] starts with a black ring, where the metric in the interior is just the classically expected one (similar in spirit to Fig.1(a) for a black hole). Momentum is then added to this metric by boosting. But we have argued that such an interior metric is *not* a correct description for the region inside the horizon; this region we believe is very nontrivial, with details that necessarily depend on the particular state which the system takes (out of the e^S possible states). In our construction in the present paper, we started with a particular state (for the extremal D1-D5) and then we were indeed able to add a unit of momentum.¹³

We can emphasize this point in another way, without bringing the third charge into the argument. Suppose we start with the *naive* metric for the *nonextremal* F string. This metric will have cylindrical symmetry around the axis of the F string. We can boost and add momentum, still keeping the cylindrical symmetry and getting F and P charges. We can then take the non-extremality to zero. This process will reproduce the *naive* metric (2.1) of the extremal FP system. To get the *correct* metrics for extremal FP starting from non-extremal FP we would have to start with one of the correct interior states for the *nonextremal* FP system.

Clearly what we need next is a construction of the generic 3-charge configuration (i.e. with the P charge not small). It is important that the solutions represent true bound states rather than just multi-center brane solutions that are classically supersymmetric. (Some families of metrics with 3 charges have been constructed before (e.g. [29]) but we are not aware of any set that actually describes the bound states that we wish to study.¹⁴ It is possible that the generic state is not well approximated by a classical configuration; what we do expect though on the basis of all that was said above is that the region where the different states depart from each other will be of the order the horizon size and not just a planck sized region near the singularity.

Acknowledgements

This work was supported in part by DOE grant DE-FG02-91ER-40690. We are grateful to Oleg Lunin for many helpful discussions, and for several contributions in the initial stages

¹³One should not use the ‘correspondence principle’ [28] to obtain a qualitative understanding of what might happen inside horizons. It was shown in [25] that at coupling $g < g_c$ the energy added to a string goes to exciting vibrations, while at $g > g_c$ the energy goes to creating *brane-antibrane pairs*. (Here g_c is the coupling at the ‘correspondence point’ where the string turns to a black hole.) It is these brane-antibrane pairs that have the small energy gaps and large phase space to ‘fill up’ the interior of the horizon.

¹⁴We thank D. Mateos and O. Lunin for discussions on this point.

of this project. We also thank Jan de Boer, Sumit Das, Steven Giddings, Per Kraus, David Kutasov, Emil Martinec and David Mateos for useful comments and discussions.

Appendix A: Spherical Harmonics on S^3

In this Appendix we list the explicit forms of the various spherical harmonics encountered in the solutions. The metric on the unit 3-sphere is

$$ds^2 = d\theta^2 + \cos^2 \theta d\psi^2 + \sin^2 \theta d\phi^2 \quad (\text{A.1})$$

The harmonics will be orthonormal

$$\begin{aligned} \int d\Omega (Y^{I_1})^* Y^{I'_1} &= \delta^{I_1, I'_1} \\ \int d\Omega (Y_a^{I_3})^* Y^{I'_3 a} &= \delta^{I_3, I'_3} \end{aligned} \quad (\text{A.2})$$

In order to simplify notation we have used the following abbreviations

$$\hat{Y}^{(l)} \equiv Y_{(l,l)}^{(l,l)} \quad (\text{A.3})$$

$$Y^{(l)} \equiv Y_{(l-1,l)}^{(l,l)} \quad (\text{A.4})$$

$$Y^{(l+1)} \equiv Y_{(l-1,l)}^{(l+1,l+1)} \quad (\text{A.5})$$

$$Y_a^{(l+1,l)} \equiv Y_{a(l-1,l)}^{(l+1,l)} \quad (\text{A.6})$$

$$Y_a^{(l,l+1)} \equiv Y_{a(l-1,l)}^{(l,l+1)} \quad (\text{A.7})$$

$$Y_a^{(l-1,l)} \equiv Y_{a(l-1,l)}^{(l-1,l)} \quad (\text{A.8})$$

$$Y_a^{(l+2,l+1)} \equiv Y_{a(l-1,l)}^{(l+2,l+1)} \quad (\text{A.9})$$

$$Y_a^{(l+1,l+2)} \equiv Y_{a(l-1,l)}^{(l+1,l+2)} \quad (\text{A.10})$$

A.1 Scalar Harmonics

The scalar harmonics we use are (in explicit form)

$$\hat{Y}^{(l)} = \sqrt{\frac{2l+1}{2}} \frac{e^{-2il\phi}}{\pi} \sin^{2l} \theta \quad (\text{A.11})$$

$$Y^{(l)} = -\frac{\sqrt{l(2l+1)}}{\pi} e^{-i(2l-1)\phi + i\psi} \sin^{2l-1} \theta \cos \theta \quad (\text{A.12})$$

$$Y^{(l+1)} = \frac{\sqrt{(2l+1)(2l+3)}}{2\pi} e^{-i(2l-1)\phi + i\psi} ((l-1) + (l+1) \cos 2\theta) \sin^{2l-1} \theta \cos \theta \quad (\text{A.13})$$

A.2 Vector Harmonics

The vector harmonics are given by

$$Y_{\theta}^{(l+1,l)} = -\frac{e^{-i(2l-1)\phi+i\psi}}{4\pi} \frac{\sin^{2l-2} \theta}{\sqrt{l+1}} ((2l^2 - l + 1) + (l-1)(2l+1) \cos 2\theta) \quad (\text{A.14})$$

$$Y_{\psi}^{(l+1,l)} = i \frac{e^{-i(2l-1)\phi+i\psi}}{4\pi} \frac{\sin^{2l-1} \theta \cos \theta}{\sqrt{l+1}} ((2l^2 + 3l - 1) + (l+1)(2l+1) \cos 2\theta) \quad (\text{A.15})$$

$$Y_{\phi}^{(l+1,l)} = -i \frac{e^{-i(2l-1)\phi+i\psi}}{4\pi} \frac{\sin^{2l-1} \theta \cos \theta}{\sqrt{l+1}} ((2l^2 - 5l - 1) + (2l^2 + 3l + 1) \cos 2\theta) \quad (\text{A.16})$$

$$Y_{\theta}^{(l,l+1)} = -\frac{e^{-i(2l-1)\phi+i\psi}}{4\pi} \sqrt{\frac{4l(2l+1)}{l+1}} \sin^{2l-2} \theta ((l-1) + l \cos 2\theta) \quad (\text{A.17})$$

$$Y_{\psi}^{(l,l+1)} = i \frac{e^{-i(2l-1)\phi+i\psi}}{4\pi} \sqrt{\frac{4l(2l+1)}{l+1}} \sin^{2l-1} \theta \cos \theta (l + (l+1) \cos 2\theta) \quad (\text{A.18})$$

$$Y_{\phi}^{(l,l+1)} = i \frac{e^{-i(2l-1)\phi+i\psi}}{4\pi} \sqrt{\frac{4l(2l+1)}{l+1}} \sin^{2l-1} \theta \cos \theta ((l+2) + (l+1) \cos 2\theta) \quad (\text{A.19})$$

$$Y_{\theta}^{(l-1,l)} = \frac{e^{-i(2l-1)\phi+i\psi}}{2\pi} \sqrt{2l-1} \sin^{2l-2} \theta \quad (\text{A.20})$$

$$Y_{\psi}^{(l-1,l)} = -i \frac{e^{-i(2l-1)\phi+i\psi}}{2\pi} \sqrt{2l-1} \sin^{2l-1} \theta \cos \theta \quad (\text{A.21})$$

$$Y_{\phi}^{(l-1,l)} = -i \frac{e^{-i(2l-1)\phi+i\psi}}{2\pi} \sqrt{2l-1} \sin^{2l-1} \theta \cos \theta \quad (\text{A.22})$$

$$Y_{\theta}^{(l+2,l+1)} = -\frac{e^{-i(2l-1)\phi+i\psi}}{8\pi} \sqrt{\frac{3}{l+2}} \sin^{2l-2} \theta \left[(l-1)(2l^2 + l + 1) + \frac{2(4l^3 - l + 3) \cos 2\theta}{3} + \frac{(l-1)(l+1)(2l+3) \cos 4\theta}{3} \right] \quad (\text{A.23})$$

$$Y_{\psi}^{(l+2,l+1)} = -i \frac{e^{-i(2l-1)\phi+i\psi}}{4\pi} \sqrt{\frac{3}{l+2}} \sin^{2l-1} \theta \cos \theta \left[\frac{l(2l^2 + 5l - 1)}{2} + \frac{1}{3}(l+1)(4l^2 + 8l - 3) \cos 2\theta + \frac{(l+1)(l+2)(2l+3)}{6} \cos 4\theta \right] \quad (\text{A.24})$$

$$Y_{\phi}^{(l+2,l+1)} = i \frac{e^{-i(2l-1)\phi+i\psi}}{4\pi} \sqrt{\frac{3}{l+2}} \sin^{2l-1} \theta \cos \theta \left[\frac{(2l^3 - 3l^2 + 3l + 4)}{2} + \frac{1}{3}(4l^3 - 13l - 9) \cos 2\theta + \frac{(l+1)(l+2)(2l+3)}{6} \cos 4\theta \right] \quad (\text{A.25})$$

Appendix B: Solution – inner region

The supergravity equations are expressed in terms of the fields B_{MN} and w . It is convenient to divide the B_{MN} into three classes – B_{ab} , $B_{\mu a}$ and $B_{\mu\nu}$ where B_{ab} is an antisymmetric tensor on S^3 , $B_{\mu a}$ is a vector on S^3 and $B_{\mu\nu}$ is a scalar on S^3 . At a given order ϵ^n , the corrections to B_{ab} and $B_{\mu\nu}$ at that order can be expressed in terms of a single scalar field b and the antisymmetric tensor $t_{\mu\nu}$:

$$B_{ab} = \epsilon_{abc} e^{-2il\frac{a}{Q}t} \partial^c b \quad (\text{B.1})$$

$$B_{\mu\nu} = \frac{r}{Q} \tilde{\epsilon}_{\mu\nu\lambda} \partial^\lambda \left(e^{-2il\frac{a}{Q}t} b \right) + e^{-2il\frac{a}{Q}t} t_{\mu\nu} \quad (\text{B.2})$$

Here ϵ_{abc} is the usual Levi-Civita tensor on the unit S^3 (with $\epsilon_{\theta\psi\phi} = \sqrt{g}$), while $\tilde{\epsilon}_{\mu\nu\lambda}$ is the Levi-Civita tensor *density* on the t, y, r part of the metric (2.20); thus $\tilde{\epsilon}_{tyr} = 1$. Below we will give the values of b and $t_{\mu\nu}$ at each order in the perturbation. The 1-forms B_{ta} , B_{ya} and B_{ra} will be given explicitly. To avoid cumbersome notation we do not put labels on the fields indicating the order of perturbation; rather we list the order of all fields in the subsection heading.

In this Appendix the solutions are in the NS sector coordinates. In order to compare with the outside we need to spectral flow these to the R sector using the coordinate transformation

$$\psi_{NS} = \psi - \frac{a}{Q}y, \quad \phi_{NS} = \phi - \frac{a}{Q}t \quad (\text{B.3})$$

The perturbation expansion in the NS sector coordinates has only even powers of ϵ . The spectral flow (B.3) to R sector coordinates generates odd powers in ϵ . Thus the $O(\epsilon^0)$ NS sector computation gives $O(\epsilon^0), O(\epsilon^1)$ in the R coordinates.

The solution to a given order ϵ^n is given by the sum of the corrections at all orders $\leq n$.

B.1 Leading Order ($O(\epsilon^0) \rightarrow O(\epsilon^0), O(\epsilon^1)$)

$$b = \frac{1}{4l} \frac{1}{(r^2 + a^2)^l} Y_{NS}^{(l)} \quad (\text{B.4})$$

$$w = \frac{1}{Q(r^2 + a^2)^l} Y_{NS}^{(l)} e^{-2il\frac{a}{Q}t} \quad (\text{B.5})$$

$$B_{ta} = B_{ya} = B_{ra} = 0 \quad (\text{B.6})$$

$$t_{\mu\nu} = 0 \quad (\text{B.7})$$

B.2 Second Order ($O(\epsilon^2) \rightarrow O(\epsilon^2), O(\epsilon^3)$)

$$b = \frac{a^2}{Q(r^2 + a^2)^l} \left[\frac{(3l-1) - 2l(l+1)\cos^2\theta}{4l(l+1)^2} \right] Y_{NS}^{(l)} \quad (\text{B.8})$$

$$w = -\frac{1}{Q(r^2 + a^2)^l} \frac{r^2 + a^2 \cos^2\theta}{Q} Y_{NS}^{(l)} e^{-2il\frac{a}{Q}t} \quad (\text{B.9})$$

$$\begin{aligned} B_{ta} = & -\frac{ia}{Q^2(r^2 + a^2)^l} \left[\left(\sqrt{\frac{l}{(l+1)^5(2l+1)}} \right) [(2l+1)a^2 + (l+1)^2r^2] (Y_a^{(l+1,l)})_{NS} \right. \\ & + \left(\frac{1}{2(l+1)^2} \sqrt{\frac{1}{(l+1)}} \right) [(3l+1)a^2 + (l+1)^2r^2] (Y_a^{(l,l+1)})_{NS} \\ & \left. - \left(\frac{1}{4l} \sqrt{\frac{2l-1}{l(2l+1)}} \right) [a^2 + 2lr^2] (Y_a^{(l-1,l)})_{NS} \right] e^{-2il\frac{a}{Q}t} \end{aligned} \quad (\text{B.10})$$

$$\begin{aligned} B_{ya} = & -\frac{ia}{Q^2(r^2 + a^2)^l} \left[\left(\sqrt{\frac{l}{(l+1)(2l+1)}} \right) r^2 (Y_a^{(l+1,l)})_{NS} - \frac{1}{2\sqrt{l+1}} r^2 (Y_a^{(l,l+1)})_{NS} \right. \\ & \left. - \left(\frac{1}{4l} \sqrt{\frac{2l-1}{l(2l+1)}} \right) [a^2 + 2lr^2] (Y_a^{(l-1,l)})_{NS} \right] e^{-2il\frac{a}{Q}t} \end{aligned} \quad (\text{B.11})$$

$$\begin{aligned} B_{ra} = & \frac{a^2}{Q(r^2 + a^2)^{l+1}} \left[\left(\sqrt{\frac{l^5}{(l+1)^5(2l+1)}} \right) r (Y_a^{(l+1,l)})_{NS} + \left(\frac{l(l-1)}{2(l+1)^{\frac{5}{2}}} \right) r (Y_a^{(l,l+1)})_{NS} \right. \\ & \left. - \left(\frac{1}{4l} \sqrt{\frac{2l-1}{l(2l+1)}} \right) \frac{1}{r} [a^2 + 2lr^2] (Y_a^{(l-1,l)})_{NS} \right] e^{-2il\frac{a}{Q}t} \end{aligned} \quad (\text{B.12})$$

$$t_{ty} = \frac{r^2}{Q^3(r^2 + a^2)^l} \left[\left(\frac{(2l+1)a^2 + (l+1)^2r^2}{(l+1)^2} \right) Y_{NS}^{(l)} + a^2 \frac{l}{(l+1)^2} \sqrt{\frac{l}{(2l+3)}} Y_{NS}^{(l+1)} \right] \quad (\text{B.13})$$

$$\begin{aligned} t_{yr} = & i \frac{ar}{Q^2(r^2 + a^2)^{l+1}} \left(\frac{(l^2 + 2l - 1)a^2 - (l^2 - 1)(2l - 1)r^2}{2l(l+1)^2} \right) Y_{NS}^{(l)} \\ & - i \frac{a^3r}{Q^2(r^2 + a^2)^{l+1}} \frac{l}{(l+1)^2} \sqrt{\frac{l}{(2l+3)}} Y_{NS}^{(l+1)} \end{aligned} \quad (\text{B.14})$$

$$t_{tr} = i \frac{ar}{Q^2(r^2 + a^2)^l} \frac{l-1}{2l(l+1)} Y_{NS}^{(l)} \quad (\text{B.15})$$

Appendix C: Solution – outer region

As was done for the inner region, we divide the field B_{MN} into three classes – B_{ab} , $B_{\mu a}$ and $B_{\mu\nu}$. At a given order ϵ^n , the corrections to B_{ab} and $B_{\mu\nu}$ at that order can be expressed in terms of a single scalar field b and the antisymmetric tensor $t_{\mu\nu}$:

$$\begin{aligned} B_{ab} &= e^{-i\frac{a}{Q}u} \epsilon_{abc} \partial^c b \\ B_{\mu\nu} &= \left(\frac{r}{Q+r^2} \tilde{\epsilon}_{\mu\nu\lambda} \partial^\lambda b + t_{\mu\nu} \right) e^{-i\frac{a}{Q}u} \end{aligned} \quad (\text{C.1})$$

Again ϵ_{abc} is the Levi-Civita tensor on the unit S^3 while $\tilde{\epsilon}_{\mu\nu\lambda}$ is the Levi-Civita tensor *density* on the t, y, r part of the metric (2.22); thus $\tilde{\epsilon}_{tyr} = 1$. We give $b, t_{\mu\nu}$ at each order. We also write

$$\begin{aligned} B_{\mu a} &= e^{-i\frac{a}{Q}u} b_{\mu a} \\ w &= e^{-i\frac{a}{Q}u} \tilde{w} \end{aligned} \quad (\text{C.2})$$

We will give $b_{\mu a}, \tilde{w}$ at each order.

The solution to a given order ϵ^n is given by the sum of the corrections at all orders $\leq n$.

C.1 Leading Order ($O(\epsilon^0)$)

$$b = \frac{1}{4l} \frac{1}{r^{2l}} Y^{(l)} \quad (\text{C.3})$$

$$\tilde{w} = \frac{1}{r^{2l}(Q+r^2)} Y^{(l)} \quad (\text{C.4})$$

$$b_{ta} = b_{ya} = b_{ra} = 0 \quad (\text{C.5})$$

$$t_{\mu\nu} = 0 \quad (\text{C.6})$$

C.2 First Order ($O(\epsilon^1)$)

$$b = \tilde{w} = 0 \quad (\text{C.7})$$

$$\begin{aligned} b_{ua} &= \frac{ia}{2} \sqrt{\frac{l}{(2l+1)(l+1)}} \frac{Q}{r^{2l}(Q+r^2)^2} Y_a^{(l+1,l)} \\ &\quad - \frac{ia}{4} \frac{1}{r^{2l}} \sqrt{\frac{2l-1}{l(2l+1)}} \frac{Q}{(Q+r^2)^2} Y_a^{(l-1,l)} + \frac{ia}{4Qr^{2l}} \sqrt{\frac{4l^2-1}{l^3}} Y_a^{(l-1,l)} \end{aligned} \quad (\text{C.8})$$

$$b_{va} = i\frac{a}{4} \sqrt{\frac{1}{(l+1)}} \frac{Q}{r^{2l}(Q+r^2)^2} Y_a^{(l,l+1)} \quad (\text{C.9})$$

$$t_{ty} = 0 \quad (C.10)$$

$$t_{rt} = ia \left(\frac{Q}{r^{2l+1}(Q+r^2)^3} \frac{[(l+2)r^2 + lQ]}{4l(l+1)} - \frac{1}{4lQr^{2l+1}} \right) Y^{(l)} \quad (C.11)$$

$$t_{yr} = ia \left(\frac{(2l-1)Q}{r^{2l+1}(Q+r^2)^3} \frac{[(l+2)r^2 + lQ]}{4l(l+1)} + \frac{1}{4lQr^{2l+1}} \right) Y^{(l)} \quad (C.12)$$

$$(C.13)$$

C.3 Second Order ($O(\epsilon^2)$)

$$b = \frac{a^2}{r^{2l}} \left(-\frac{1}{4r^2} + \frac{2Q+r^2}{(Q+r^2)^2} \left(\frac{(3l-1) - 2l(l+1)\cos^2\theta}{8l(l+1)^2} \right) \right) Y^{(l)} \quad (C.14)$$

$$\tilde{w} = \frac{a^2}{r^{2l}(Q+r^2)} \left(-\frac{l}{r^2} - \frac{\cos^2\theta}{(Q+r^2)} \right) Y^{(l)} \quad (C.15)$$

$$b_{ra} \equiv b_r^{I_3} Y_a^{I_3} = \frac{a^2}{2r^{2l+1}(Q+r^2)^3} (2l^2Q^2 + 3l(l+1)Qr^2 + l(l+1)r^4) \\ \times \left[\frac{\sqrt{l}Y_a^{(l+1,l)}}{\sqrt{(2l+1)(l+1)^5}} + \frac{l-1}{2l(l+1)^{\frac{5}{2}}} Y_a^{(l,l+1)} - \frac{1}{2l^2} \sqrt{\frac{2l-1}{l(2l+1)}} Y_a^{(l-1,l)} \right] \quad (C.16)$$

$$b_{ua} = b_{va} = 0 \quad (C.17)$$

$$t_{ty} = -\frac{a^2}{4l(l+1)^2r^{2l}(Q+r^2)^5} [l(l+1)(2l+3)Q^3 \\ + l(6l^2 + 9l + 7)Q^2r^2 + (6l^3 + 4l^2 + l + 3)Qr^4 + (2l^3 - l + 1)r^6] Y^{(l)} \\ + \frac{a^2Q}{2r^{2l}(l+1)^2(Q+r^2)^5} \sqrt{\frac{l}{2l+3}} [(l+1)Q^2 + (3l+1)Qr^2 + 2(l+1)r^4] Y^{(l)} \quad (C.18)$$

$$t_{yr} = 0, \quad t_{rt} = 0 \quad (C.19)$$

C.4 Third Order ($O(\epsilon^3)$)

$$b = \tilde{w} = b_{ra} = 0 \quad (C.20)$$

$$\begin{aligned} b_{ua} = & \left(\frac{ia^3 Q}{2(Q+r^2)^3 r^{2l}(l+1)(2l+3)} \sqrt{\frac{3l(2l+1)}{l+2}} \right) Y_a^{(l+2, l+1)} \\ & + \left(\frac{ia^3 Q}{2(Q+r^2)^2 r^{2l}(l+1)^{\frac{3}{2}}} \left[\frac{(l-1)(2Q+r^2)}{4Q^2(l+1)} - \frac{2l}{(2l+3)(Q+r^2)} \right] \right) Y_a^{(l, l+1)} \\ & - \frac{ia^3}{4Q(Q+r^2)^3 r^{2l+2}} \sqrt{\frac{l}{(l+1)^5(2l+1)}} \left[(4l^2+2l+4)Q^2 r^2 + (6l^2-3l)Qr^4 + \right. \\ & \left. (2l^2-l)r^6 + 2l(Q+r^2)((l+1)^2 Q^2 - 2lQr^2 - lr^4) \right] Y_a^{(l+1, l)} \\ & + \frac{ia^3}{Qr^{2l+2}} \sqrt{\frac{2l-1}{l(2l+1)}} \left(-\frac{1}{4(Q+r^2)^2} ((l+1)(Q^2+4Qr^2+2r^4)) + \frac{r^2}{4lQ} \right. \\ & \left. + \frac{r^2}{8l(l+1)(Q+r^2)^3} (2(2l^2+3l-1)Q^2 + (3Qr^2+r^4)(2l^2+l-1)) \right) Y_a^{(l-1, l)} \end{aligned} \quad (C.21)$$

$$\begin{aligned} b_{va} = & - \left(\frac{iQa^3}{2(Q+r^2)^3 r^{2l}} \sqrt{\frac{l(2l+1)}{l+1}} \frac{1}{(2l+3)(l+1)} \right) Y_a^{(l+1, l)} \\ & - \left(\frac{iQa^3}{8\sqrt{(l+1)^3}(Q+r^2)^3 r^{2l+2}} [2l(l+1)Q + ((l+1) + (2l^2+l+3))r^2] \right) Y_a^{(l, l+1)} \\ & + \left(\frac{iQa^3}{2(Q+r^2)^3 r^{2l}} \frac{1}{(2l+3)} \sqrt{\frac{4l}{(l+1)(l+2)}} \right) Y_a^{(l+1, l+2)} \end{aligned} \quad (C.22)$$

$$\begin{aligned} t_{yr} = & - \left(\frac{ia^3 Q(2l-1)(lQ+(l+3)r^2)}{r^{2l+1}(Q+r^2)^4 l(l+1)^2} + \frac{ia^3}{4r^{2l+3}Q(Q+r^2)^3 l} \times \right. \\ & \left. \left[(l+1)(Q+r^2)^3 + l(2l-1)Q^3 + \frac{l(2l-1)(l+3)Q^2 r^2}{l+1} \right] \right) Y^{(l)} \\ & + \frac{ia^3 Q(lQ+(l+3)r^2)}{2r^{2l+1}(Q+r^2)^4} \left(\frac{(2l-1)}{(l+1)^2(l+2)} \sqrt{\frac{l}{(2l+3)}} \right) Y^{(l+1)} \end{aligned} \quad (C.23)$$

$$\begin{aligned}
t_{rt} = & \left(-\frac{ia^3 Q (lQ + (l+3)r^2)}{r^{2l+1}(Q+r^2)^4 l(l+1)^2} + \frac{ia^3}{4r^{2l+3}Q(Q+r^2)^3} \times \right. \\
& \left. \left[1 - \frac{((l^2-1)Q^3 + (l^2-3)Q^2r^2 - 3(l+1)Qr^4 - (l+1)r^6)}{l(l+1)(Q+r^2)^3} \right] \right) Y^{(l)} \\
& + \left(\frac{ia^3 Q (lQ + (l+3)r^2)}{2r^{2l+1}(Q+r^2)^4} \frac{1}{(l+1)^2(l+2)} \sqrt{\frac{l}{(2l+3)}} \right) Y^{(l+1)} \quad (C.24)
\end{aligned}$$

$$t_{ty} = 0 \quad (C.25)$$

References

- [1] A. Strominger and C. Vafa, Phys. Lett. B **379**, 99 (1996), hep-th/9601029.
- [2] C. G. Callan and J. M. Maldacena, Nucl. Phys. B **472**, 591 (1996) hep-th/9602043.
- [3] L. Susskind, arXiv:hep-th/9309145.
- [4] C. Vafa, (unpublished)
- [5] A. Sen, Nucl. Phys. B **440**, 421 (1995) [arXiv:hep-th/9411187]; A. Sen, Mod. Phys. Lett. A **10**, 2081 (1995) [arXiv:hep-th/9504147].
- [6] J. M. Maldacena, Adv. Theor. Math. Phys. **2**, 231 (1998), Int. J. Theor. Phys. **38**, 1113 (1999), hep-th/9711200;
S. S. Gubser, I. R. Klebanov and A. M. Polyakov, Phys. Lett. B **428**, 105 (1998), hep-th/9802109;
E. Witten, Adv. Theor. Math. Phys. **2**, 253 (1998), hep-th/9802150.
- [7] O. Lunin and S. D. Mathur, Nucl. Phys. B **623**, 342 (2002), hep-th/0109154.
- [8] O. Lunin and S. D. Mathur, Phys. Rev. Lett. **88**, 211303 (2002), hep-th/0202072.
- [9] M. Cvetič and D. Youm, Nucl. Phys. B **476**, 118 (1996) [arXiv:hep-th/9603100];
D. Youm, Phys. Rept. **316**, 1 (1999) [arXiv:hep-th/9710046].
- [10] V. Balasubramanian, J. de Boer, E. Keski-Vakkuri and S. F. Ross, Phys. Rev. D **64**, 064011 (2001), hep-th/0011217.
- [11] J. M. Maldacena and L. Maoz, JHEP **0212**, 055 (2002) [arXiv:hep-th/0012025].
- [12] G. T. Horowitz and A. A. Tseytlin, Phys. Rev. D **51**, 2896 (1995) [arXiv:hep-th/9409021];
A. A. Tseytlin, Phys. Lett. B **381**, 73 (1996) [arXiv:hep-th/9603099].
- [13] A. Dabholkar, J. P. Gauntlett, J. A. Harvey and D. Waldram, Nucl. Phys. B **474**, 85 (1996), hep-th/9511053.

- [14] C. G. Callan, J. M. Maldacena and A. W. Peet, Nucl. Phys. B **475**, 645 (1996), hep-th/9510134.
- [15] O. Lunin and S. D. Mathur, Nucl. Phys. B **610**, 49 (2001), hep-th/0105136.
- [16] O. Lunin, J. Maldacena and L. Maoz, hep-th/0212210.
- [17] D. J. Gross and M. J. Perry, Nucl. Phys. B **226**, 29 (1983).
- [18] D. Mateos and P. K. Townsend, Phys. Rev. Lett. **87**, 011602 (2001) [arXiv:hep-th/0103030]; R. Emparan, D. Mateos and P. K. Townsend, JHEP **0107**, 011 (2001) [arXiv:hep-th/0106012].
- [19] S. Deger, A. Kaya, E. Sezgin and P. Sundell, Nucl. Phys. B **536**, 110 (1998) [arXiv:hep-th/9804166].
- [20] J. M. Maldacena and A. Strominger, JHEP **9812**, 005 (1998) [arXiv:hep-th/9804085].
- [21] O. Lunin and S. D. Mathur, Nucl. Phys. B **642**, 91 (2002) [arXiv:hep-th/0206107].
- [22] O. Lunin and S. D. Mathur, Nucl. Phys. B **615**, 285 (2001) [arXiv:hep-th/0107113].
- [23] S. R. Das and S. D. Mathur, Phys. Lett. B **375**, 103 (1996) [arXiv:hep-th/9601152].
- [24] J. M. Maldacena and L. Susskind, Nucl. Phys. B **475**, 679 (1996) [arXiv:hep-th/9604042].
- [25] S. D. Mathur, Nucl. Phys. B **529**, 295 (1998) [arXiv:hep-th/9706151].
- [26] G. T. Horowitz, J. M. Maldacena and A. Strominger, Phys. Lett. B **383**, 151 (1996) [arXiv:hep-th/9603109].
- [27] H. Elvang and R. Emparan, arXiv:hep-th/0310008.
- [28] G. T. Horowitz and J. Polchinski, Phys. Rev. D **55**, 6189 (1997) [arXiv:hep-th/9612146].
- [29] J. P. Gauntlett, R. C. Myers and P. K. Townsend, Phys. Rev. D **59**, 025001 (1999) [arXiv:hep-th/9809065].